AI for HICs

Long-Gang Pang

Central China Normal University

GuiLin, 2025-10-25

The 16th Workshop on QCD Phase Transition and Relativistic Heavy-Ion Physics (QPT 2025)

Research Background & Significance

Heavy-Ion Collision (HIC)

- Key experimental method for studying **QCD phase structure** and **nuclear matter under extreme conditions**
- Generated massive data, short life time (QGP), inverse problem

Traditional Methods

- **Low dimensional observables:** spectra, flow, statistics, correlations

Artificial Intelligence

- **State-of-the-art Pattern Recognition**, **Strong Representation Power**

Table of Contents

01

Inverse Problems

Using artificial intelligence to infer initial conditions and physical parameters of the system from observational data, solving key problems in heavy-ion collision

Initial Condition: nuclear and sub-nucleon structure, impact parameter

Nuclear phase structure, QCD EoS, Phase transition types, CEP

Hard Probes: jet energy loss, jet production positions

Inverse problems in HIC

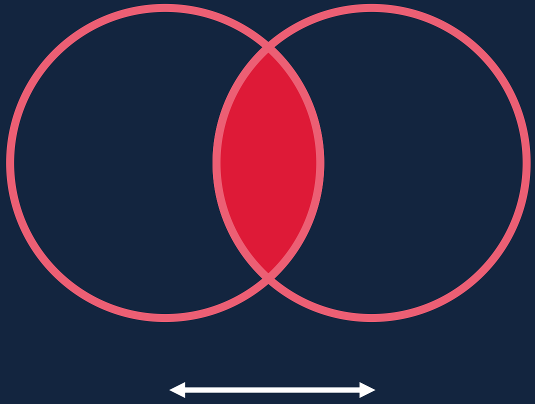

Impact parameter

S.A. Bass,A. Bischoff, J.A. Maruhn, H. Stöcker, and W. Greiner, Phys. Rev. C 53, 2358 (1996): MLP using QMD data (5*5 pz and pt distribution)

P. Xiang, Y. Zhao, X. Huang, Chi. Phys. C 53, 2358 (2022) : MLP and CNN using AMPT data

F. Li, Y. Wang, H. Lue, P. Li, Q. Li, F. Liu, JPG 47, 115104 (2020): CNN and LightGBM using UrQMD data

M. OK, J. S, K. Z, H. S, PLB 811,135872(2020): PointCloud Network using UrQMD + CBMRoot event

Inverse problems in HIC

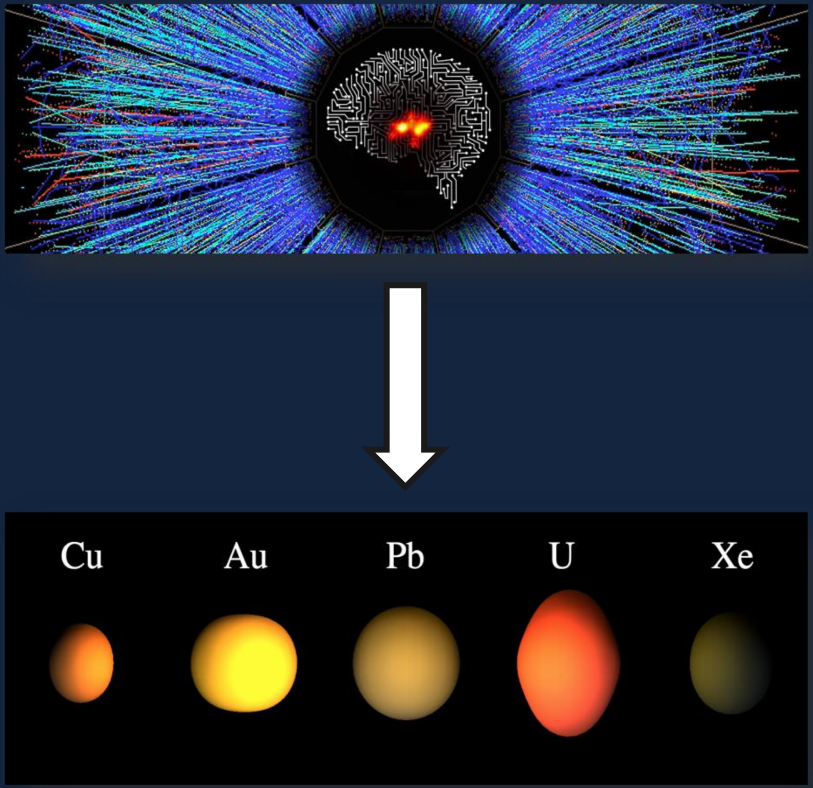

Nuclear Structure

Nuclear Structure:

1. Nuclear shape deformation
2. Alpha cluster structure
3. Nucleon-nucleon SRC, n-body correlation
4. Neutron skin thickness
5. ...

Nuclear Structure using HICs and ML

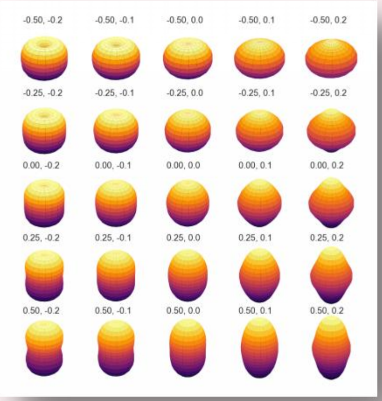

1. change β_2, β_4
2. A+A collision sim.
3. ML: final → initial nuclear deformation

LG. Pang, K. Zhou and X.-N. Wang, arXiv:1906.06429

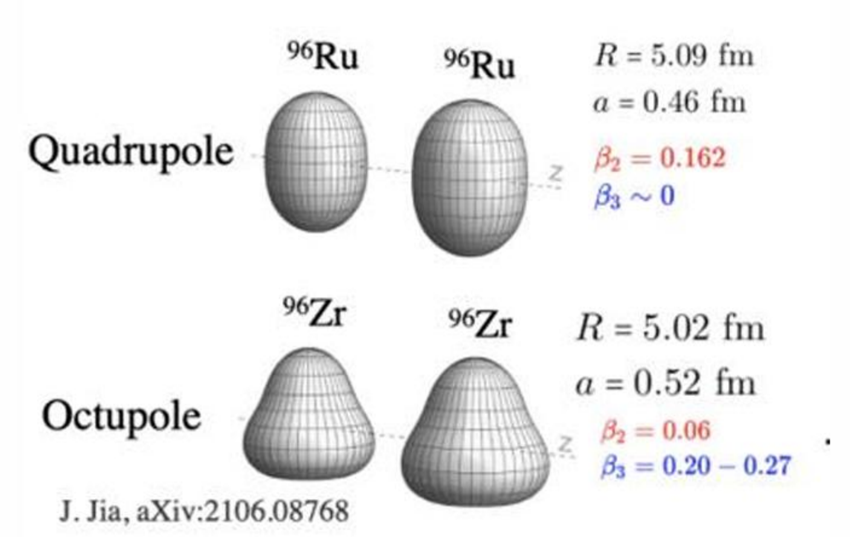

α cluster in C and O

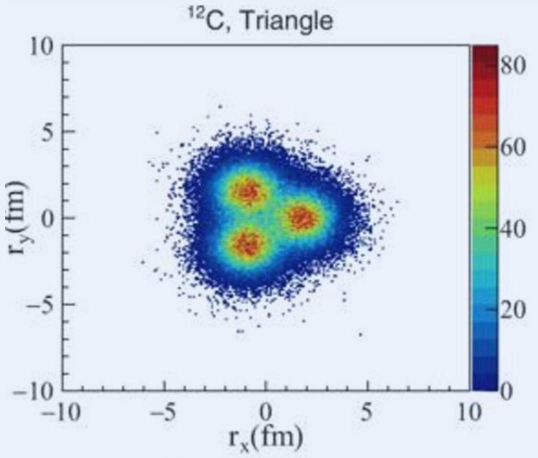

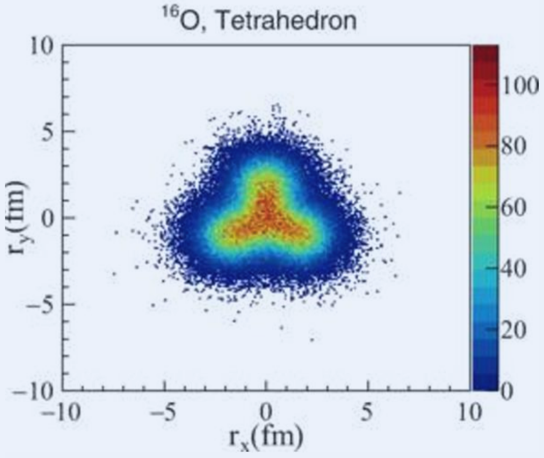

J He, W. He, Y.G. Ma, S. Zhan g, PRC104, 044902

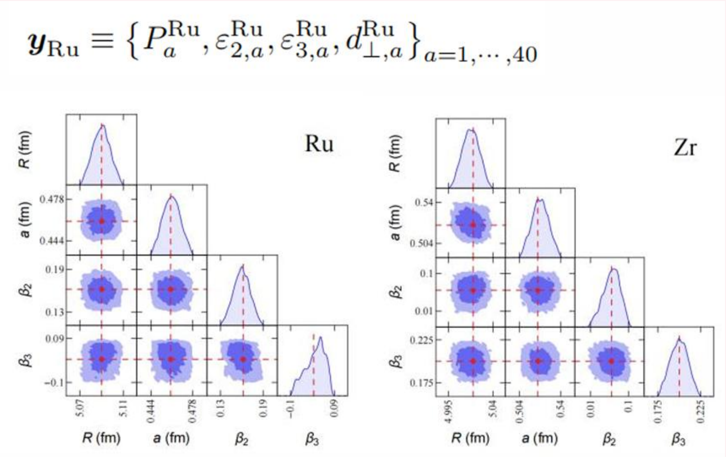

Single system works good

Y.Cheng, S.Shi, Y. Ma, H. S., K. Zhou, PRC107 (2023) 064909

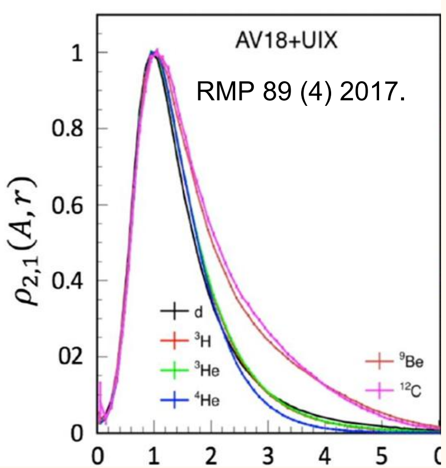

1. sample nucleons obeying both $\varrho(r)$ & $\varrho_{12}(\Delta r)$
2. do HIC simulations
3. Look for features that are sensitive to $\varrho_{12}(\Delta r)$

Y.J. Huang, Z. Meng, L.G. Pang, X.N. Wang, arXiv:2504.00790

Inverse problems in HIC

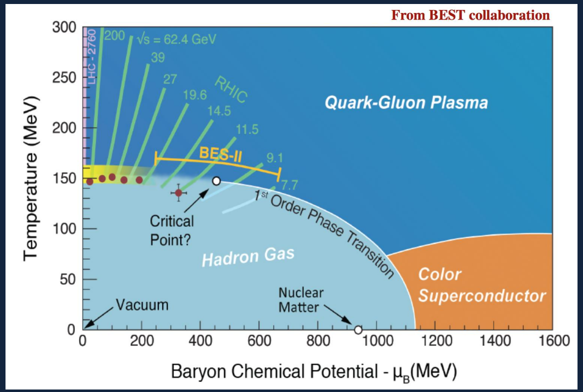

QCD Phase Structure

QCD phase structure:

1. The QCD EoS at different T, muB, muQ, muS
2. Crossover vs First order phase transition
3. The location of Critical End Point
4. The transport coefficients of hot and dense QCD matter
5. CME effects
6. Jet medium interaction, Heavy quark diffusion
7. …

Forward model: Relativistic fluid dynamics

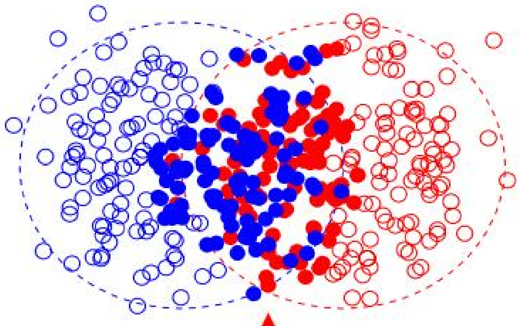

$$\nabla_\mu T^{\mu\nu} = 0$$

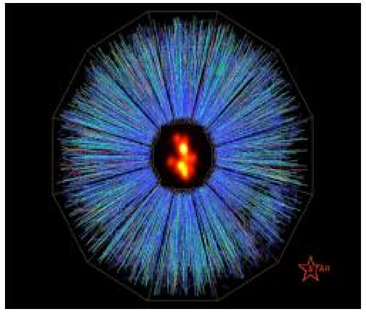

$$T^{\mu\nu} = (\varepsilon + P + \Pi)u^\mu u^\nu - (P + \Pi)g^{\mu\nu} + \pi^{\mu\nu}$$

Initial condition   EoS Bulk Viscosity   Shear Viscosity

CLVisc:

1. CCNU-LBNL Viscous Hydro, CCNU = Central China Normal University
2. A 3+1D viscous hydro parallized on GPU using OpenCL

Purpose: Describe the non-equilibrium space-time evolution of hot QCD matter
Feature: **100 times faster** than using a single core CPU.

L.G. Pang, Q. Wang and X. N. Wang, PRC 86 (2012) 024911
L.G. Pang, B.W. Xiao, Y. Hatta, X.N.Wang, PRD 2015
L.G. Pang， H.Petersen, XN Wang, PRC97(2018)no.6,064918

CLVisc for different EoS and η/s

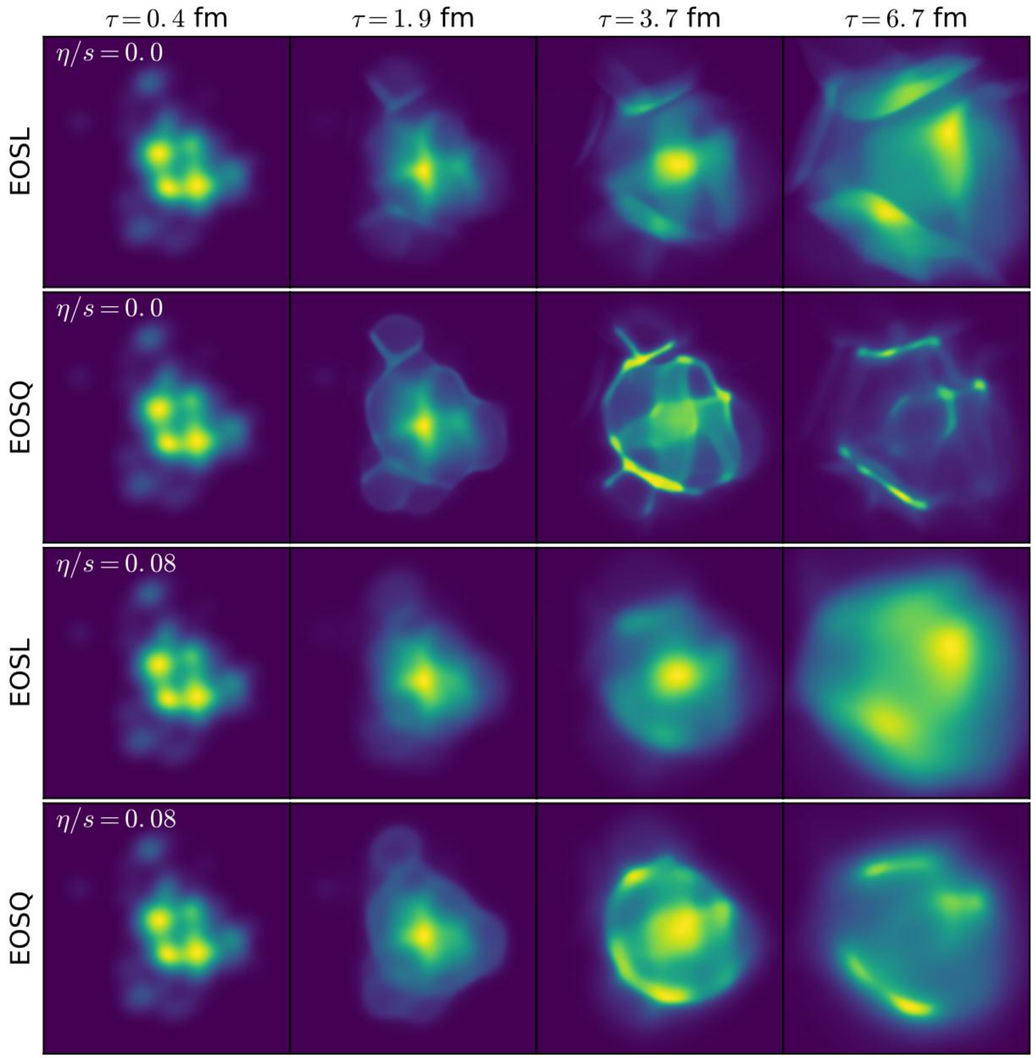

η/s = 0 (shear viscosity over entropy density)
Lattice QCD EoS (smooth cross over)

η/s = 0 (ideal hydro)
First order phase transition

η/s = 0.08 (viscous hydro)
Lattice QCD EoS (smooth cross over)

η/s = 0.08
First order phase transition

It is unknown **whether the information of EoS survives the complex dynamical evolution of HICs** and exists in each single event of the final state output.

Traditional observables (EBE)

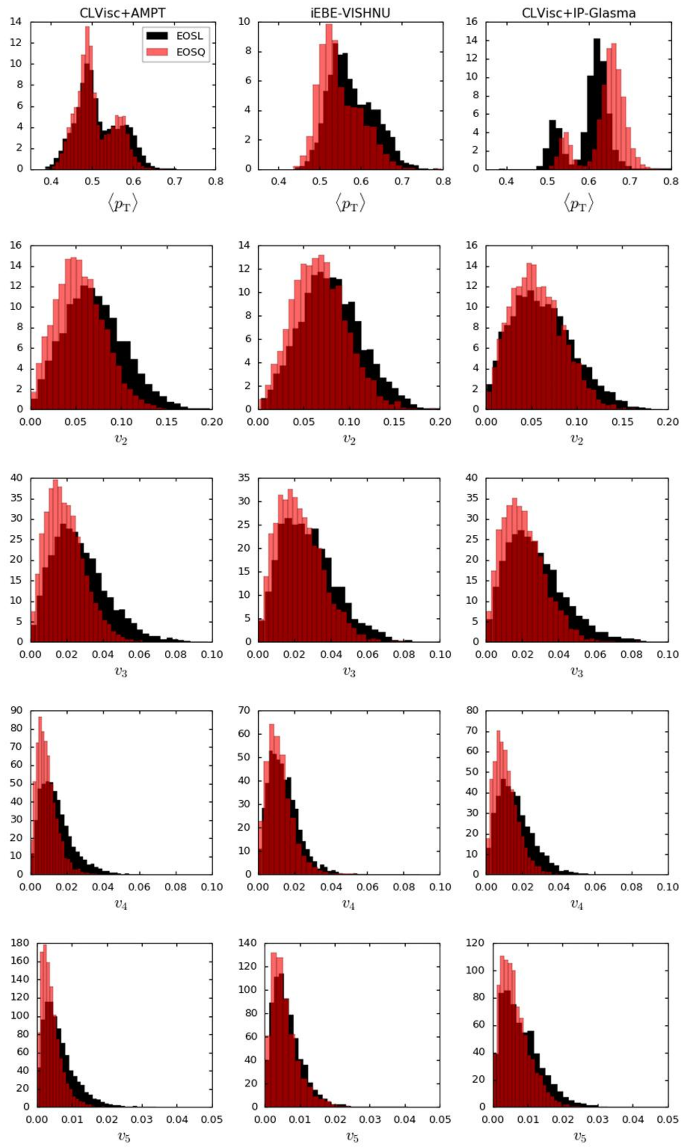

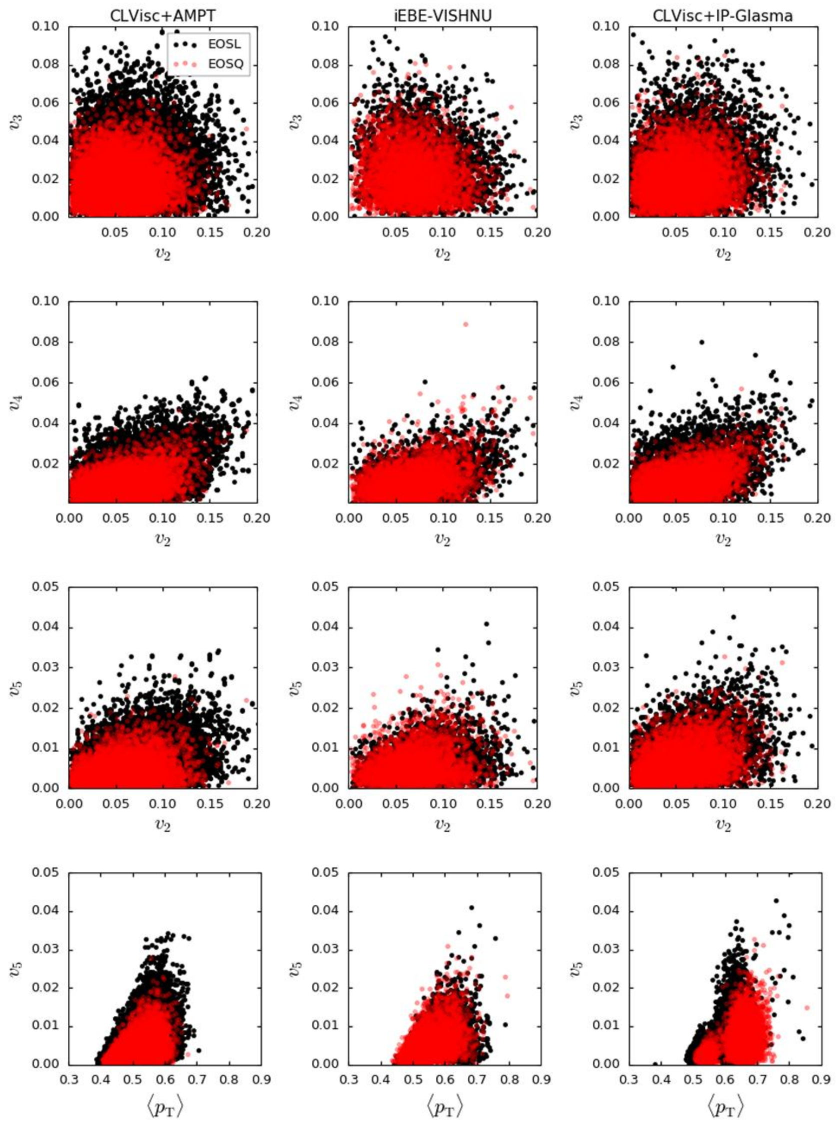

- **Challenge 1**: Significant overlap in event-by-event observables for different EoS.

- **Challenge 2**: Model-dependent biases: Mean and variance are sensitive to initial conditions and viscosity.

- **Challenge 3**: Limited separation in two-observable scattering plots.
- Key Question: Can we classify the EoS on an event-by-event basis?

DL for inverse/variational problems in HICs

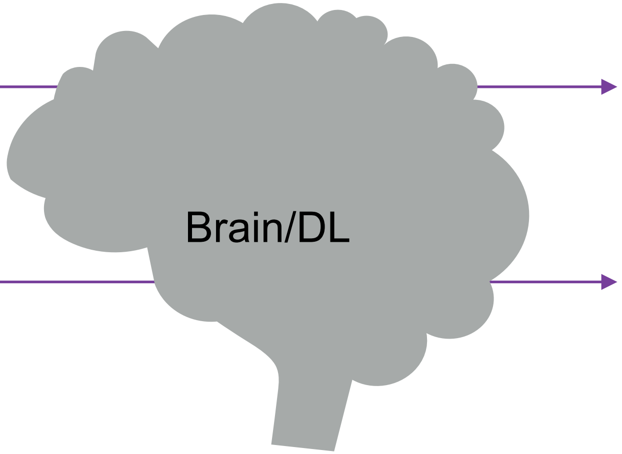

Dog

Cat

Human brains are not optimized for processing high-dimensional scientific data. Deep neural network can be trained:

(i) to identify optimal feature combinations

(ii) to represent variational functions

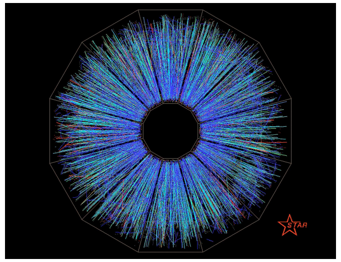

$\rho(p_T, \Phi)$

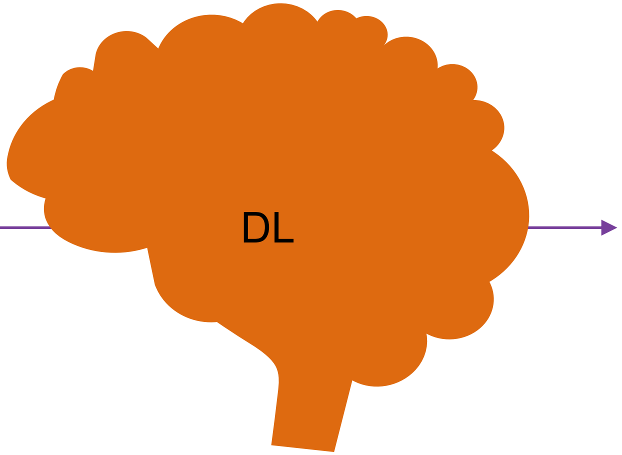

Lattce QCD EoS (crossover)

EOSQ (First order phase transition)

EoS for different phase transition types

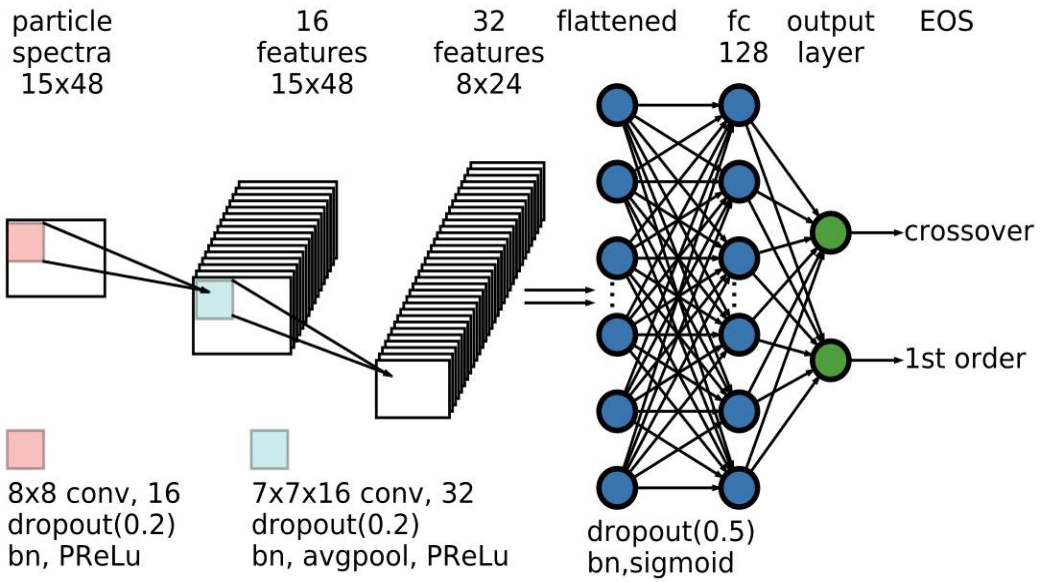

$$l(\theta) = -\frac{1}{N}\sum_{i=1}^{N}[y_i \log \hat{y}_i + (1-y_i)\log(1-\hat{y}_i)] + \lambda||\theta||_2^2$$

cross entropy loss   L2 regularization

$$\nabla_\mu T^{\mu\nu} = 0$$

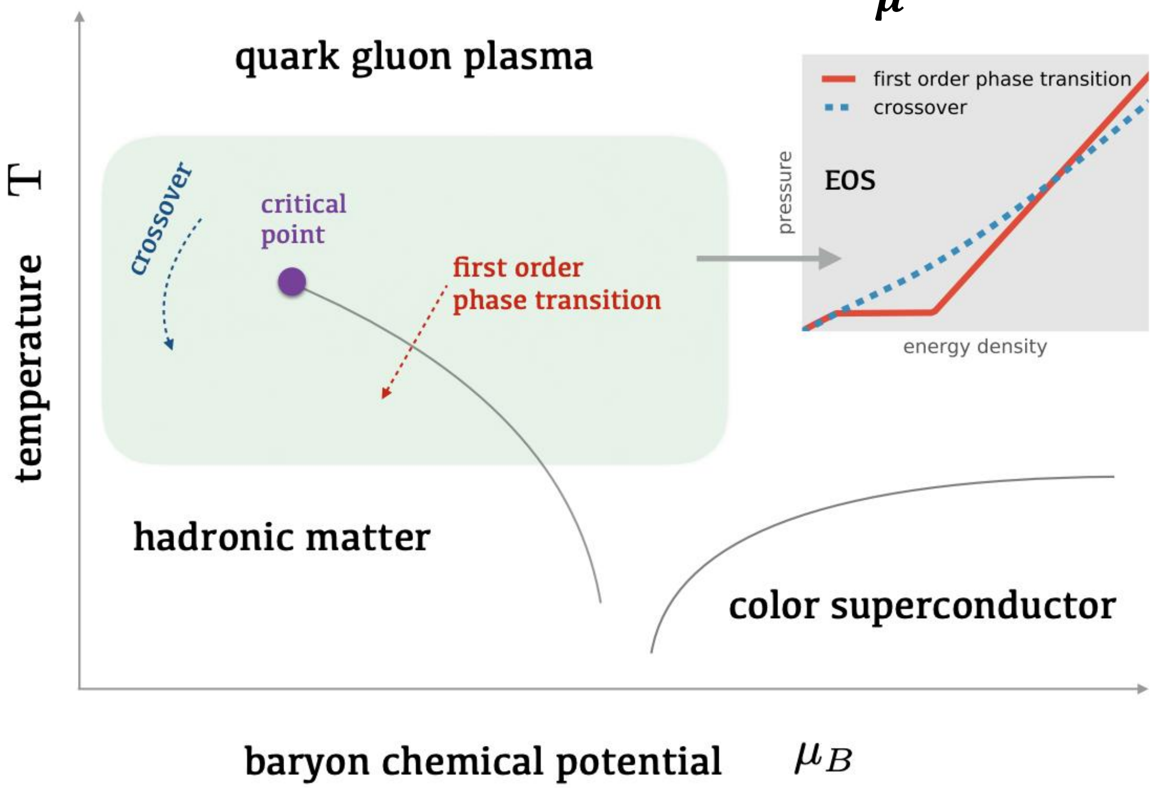

DL helps to decode the information of QCD phase transition in the QCD EoS (>93% accuracy).

Nature Communications 2018, **LG. Pang**, K.Zhou, N.Su, H.Petersen, H. Stoecker, XN. Wang.

Increasing list of ML for QCD EoS

Identifying the nature of the QCD transition in relativistic collision of heavy nuclei with deep learning, Yi-Lun Du, Kai Zhou, Jan Steinheimer, Long-Gang Pang, Anton Motornenko, Hong-Shi Zong, Xin-Nian Wang, Horst Stöcker

A machine learning study to identify spinodal clumping in high energy nuclear collisions, Jan Steinheimer, LongGang Pang, Kai Zhou, Volker Koch, Jørgen Randrup, Horst Stoecker

An equation-of-state-meter for CBM using PointNet, Manjunath Omana Kuttan, Kai Zhou, Jan Steinheimer, Andreas Redelbach, Horst Stoecker

Classification of Equation of State in Relativistic Heavy-Ion Collisions Using Deep Learning, Yu. Kvasiuk, E. Zabrodin, L. Bravina, I. Didur, M. Frolov

Neural network reconstruction of the dense matter equation of state from neutron star observables. Shriya Soma, Lingxiao Wang, Shuzhe Shi, Horst Stöcker, Kai Zhou

Learning Langevin dynamics with QCD phase transition, Lingxiao Wang, Lijia Jiang, Kai Zhou

Machine learning phase transitions of the three-dimensional Ising universality class, Xiaobing Li, Ranran Guo, Kangning Liu, Jia Zhao, Fen Long, Yu Zhou, Zhiming Li

...

Nuclear EoS at high density region

Skyrme potential + IMQMD

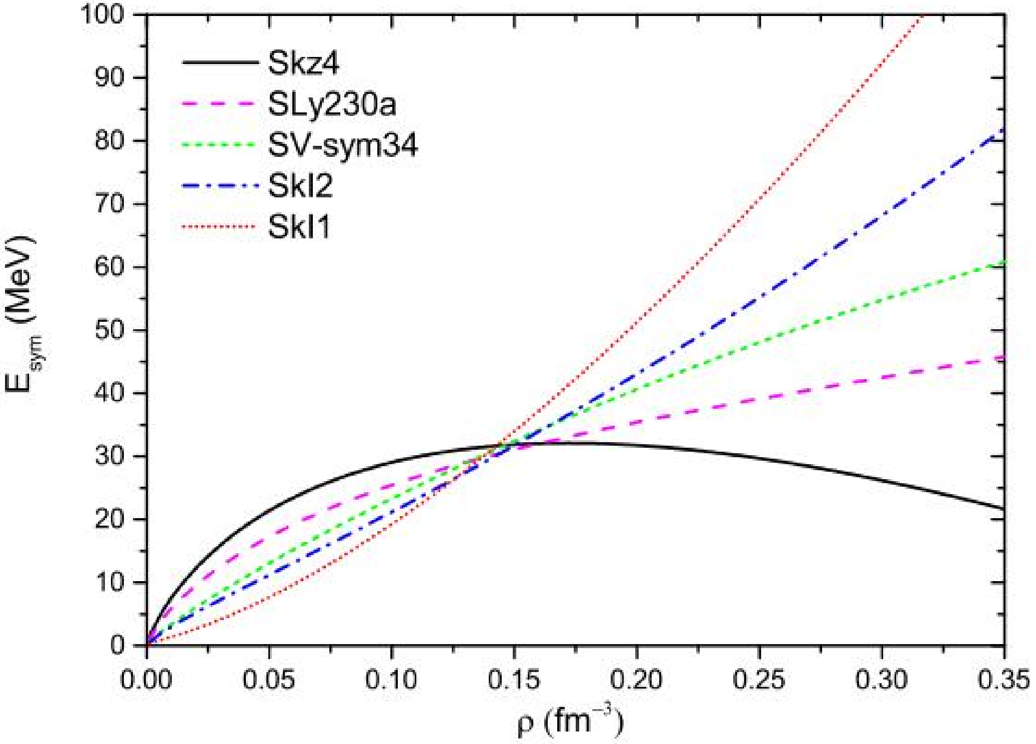

Off-diagonal = misclassified

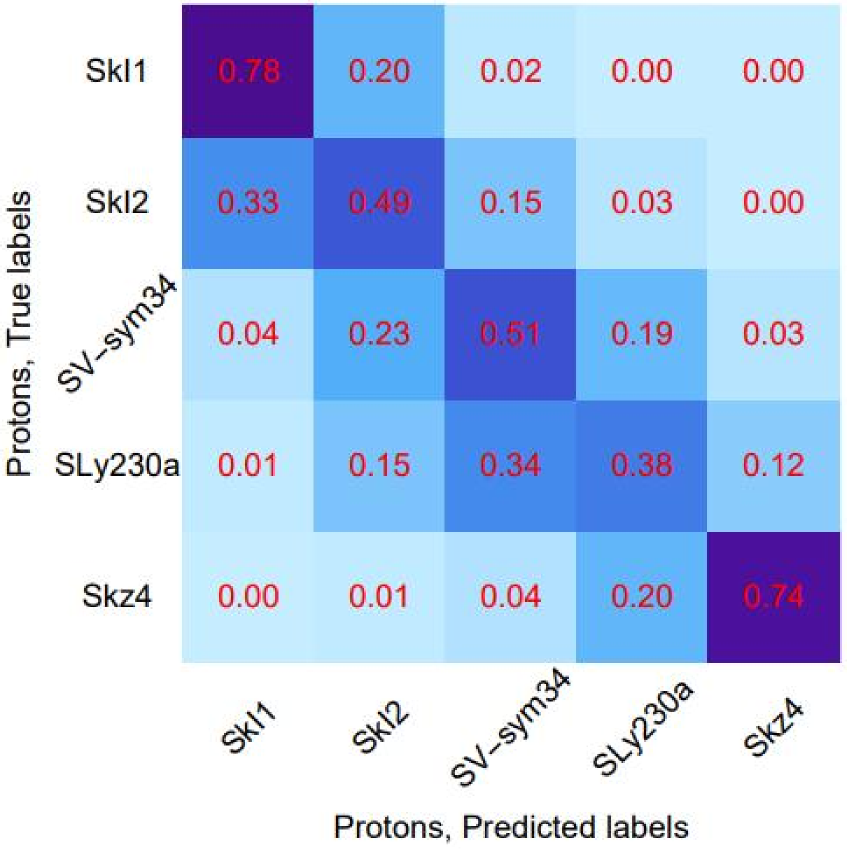

PLB 822 (2021) 136669, Y.J Wang, F.P. Li, Q.F. Li, H.L. L¨u, and K. Zhou

Auto Encoder for order parameter

PHYSICAL REVIEW RESEARCH **2**, 043202 (2020)

Nuclear liquid-gas phase transition with machine learning

Rui Wang,[1,2,*] Yu-Gang Ma,[1,2,†] R. Wada,[3] Lie-Wen Chen,[4] Wan-Bing He,[1] Huan-Ling Liu,[2] and Kai-Jia Sun[3,5]

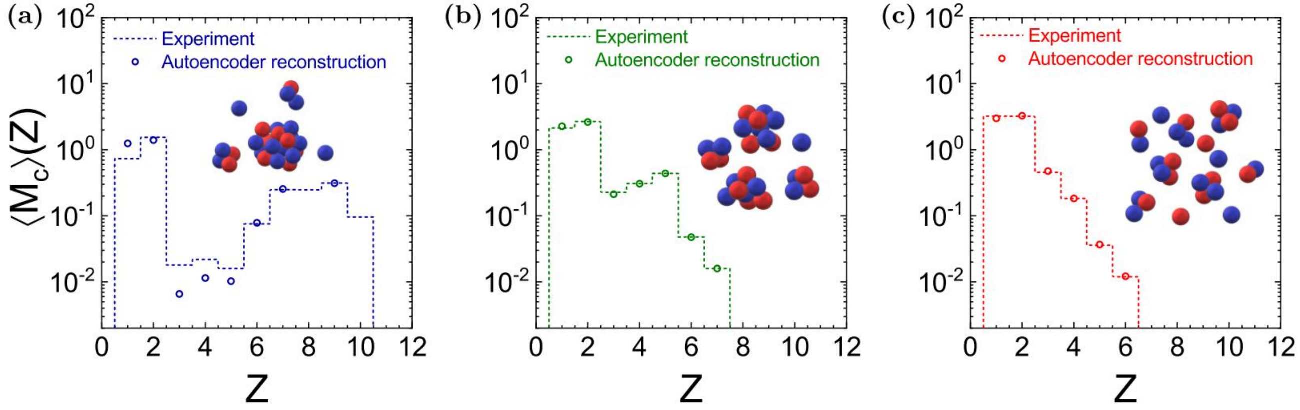

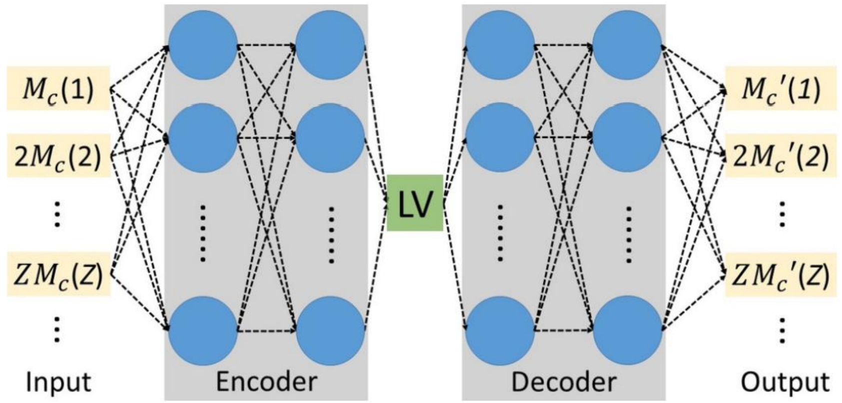

Hard Probes and medium response

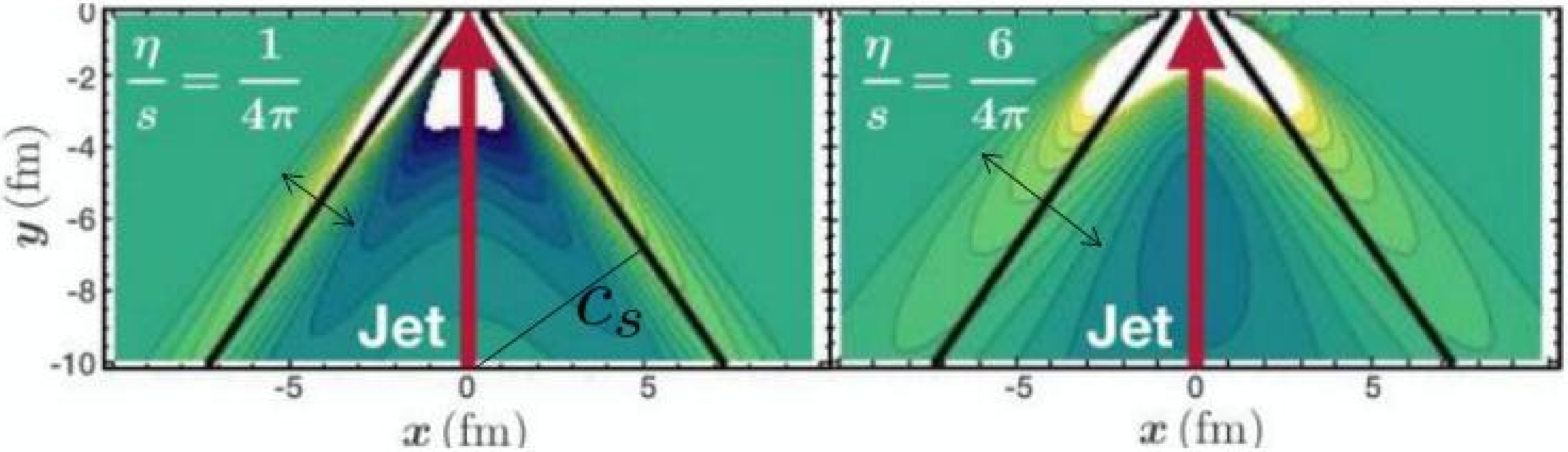

R.B.Neufeld. PRC79,054909(09')

Nuclear EoS：$c_s^2 = \frac{dP}{d\epsilon} = \sin^2\theta$

Shear Viscosity：width of the shock wave

Jet tomography with deep learning (di-jet)

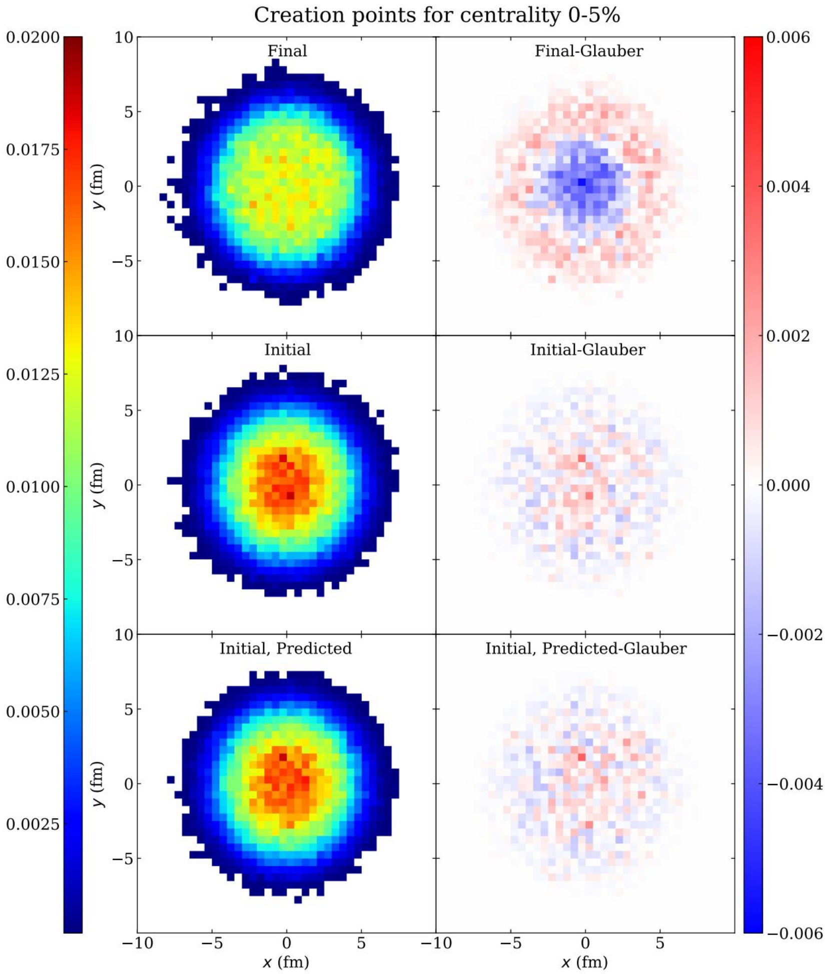

- **Top:** using final energy selection (**FES**), the estimated di-jet production point deviate from Glauber model a lot
- **Middle**: initial energy selection, **ground truth**
- **Bottom**: initial energy selection using predicted energy loss and initial jet energy **with deep learning**

YL Du, D Pablos and K Tywoniuk, PRL128, no.1, 012301 (2022)

LBT+CLVisc+DeepLearning jet tomography

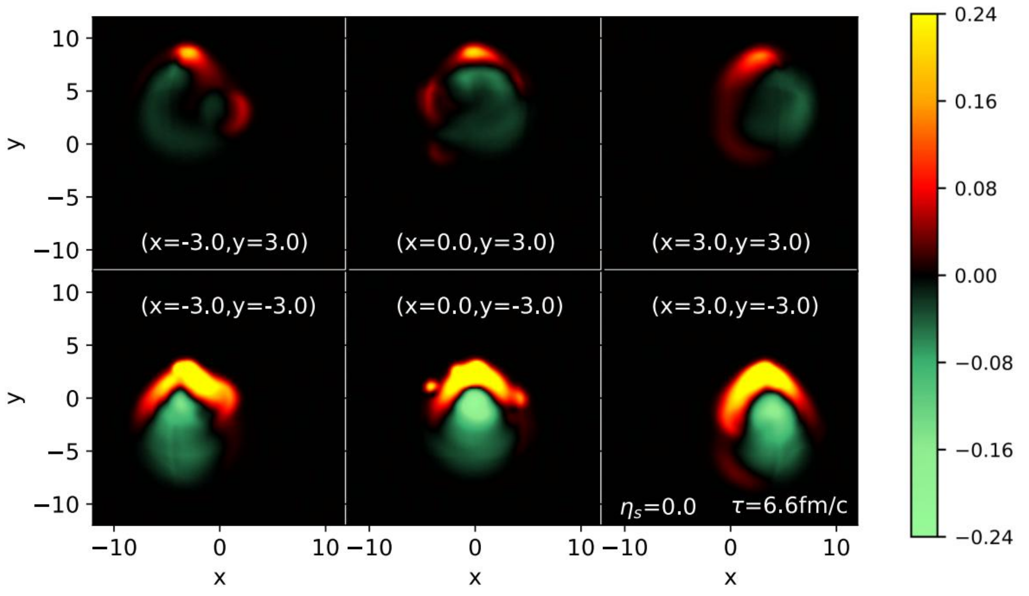

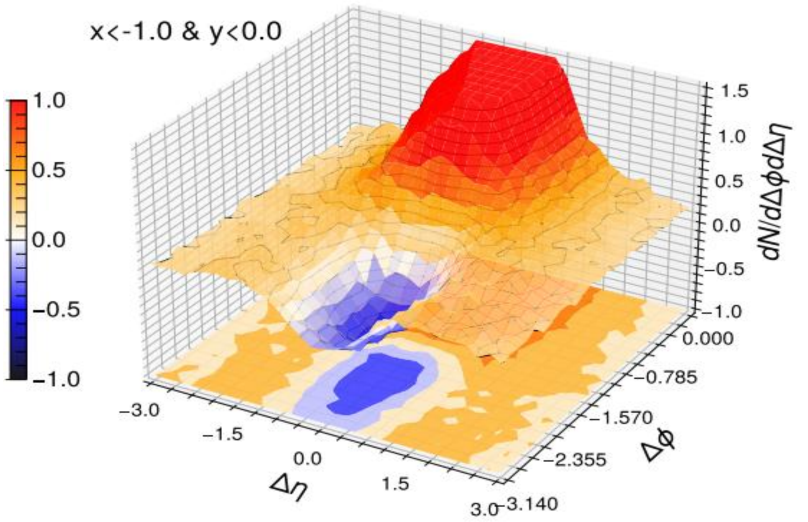

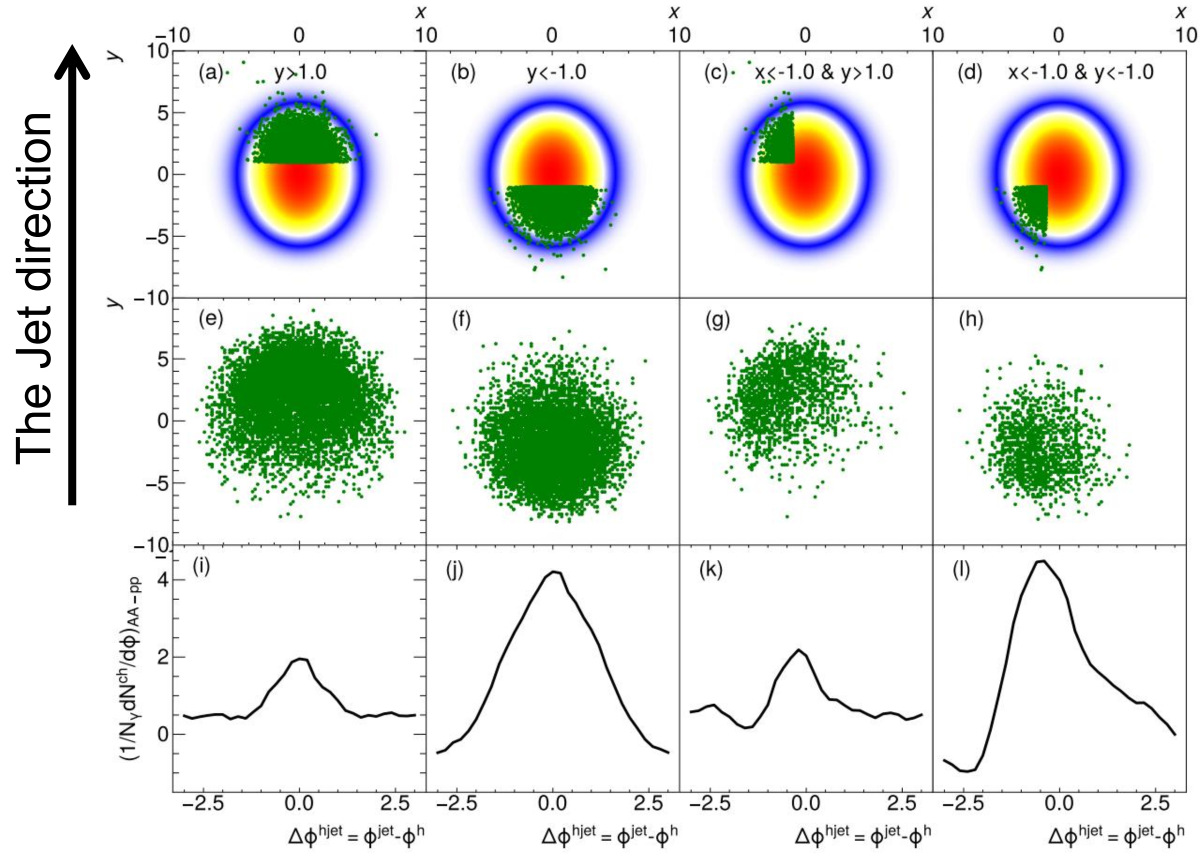

Z Yang, YY He, W Chen, WY Ke, LG Pang, XN Wang, EPJC 83 (2023) 7, 652

Z Yang, T Luo, W Chen, LG Pang, XN Wang, PRL 130 (2023) 5, 052301

Detecting CME via AMPT + CNN/UNET

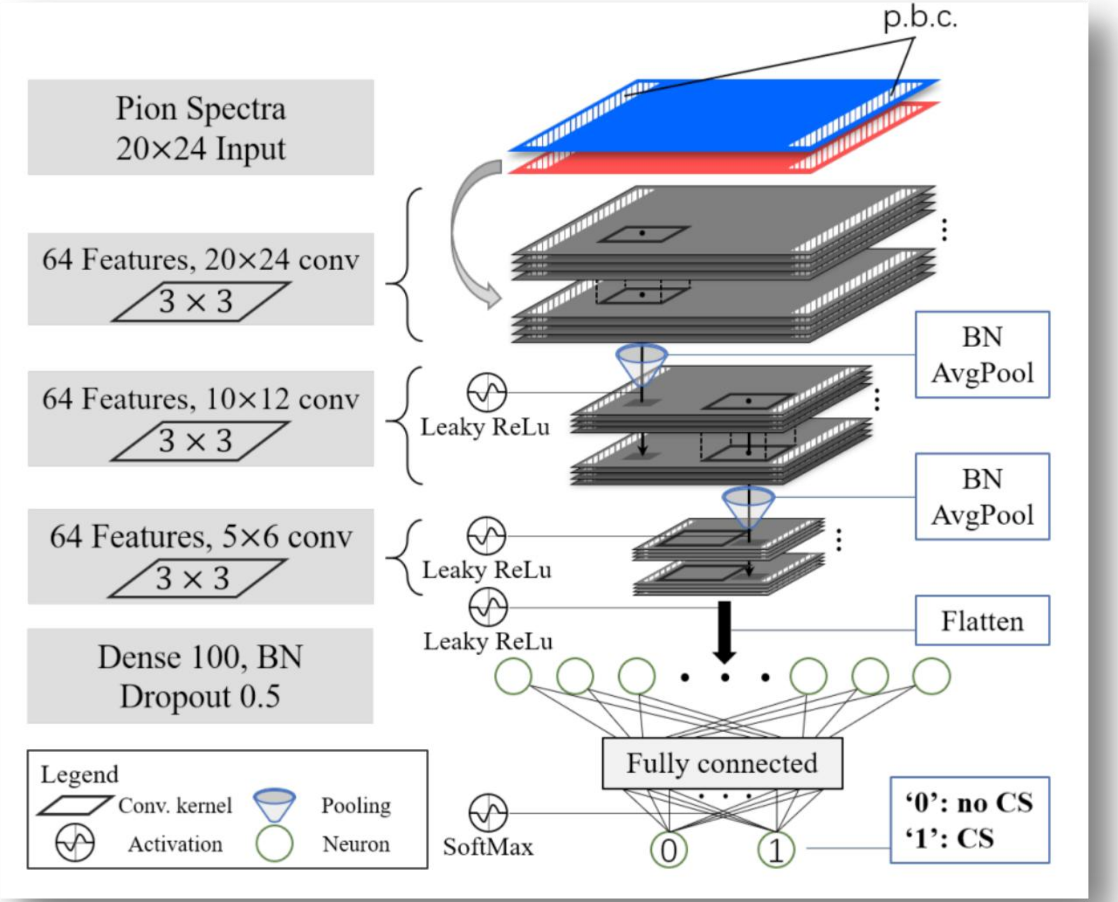

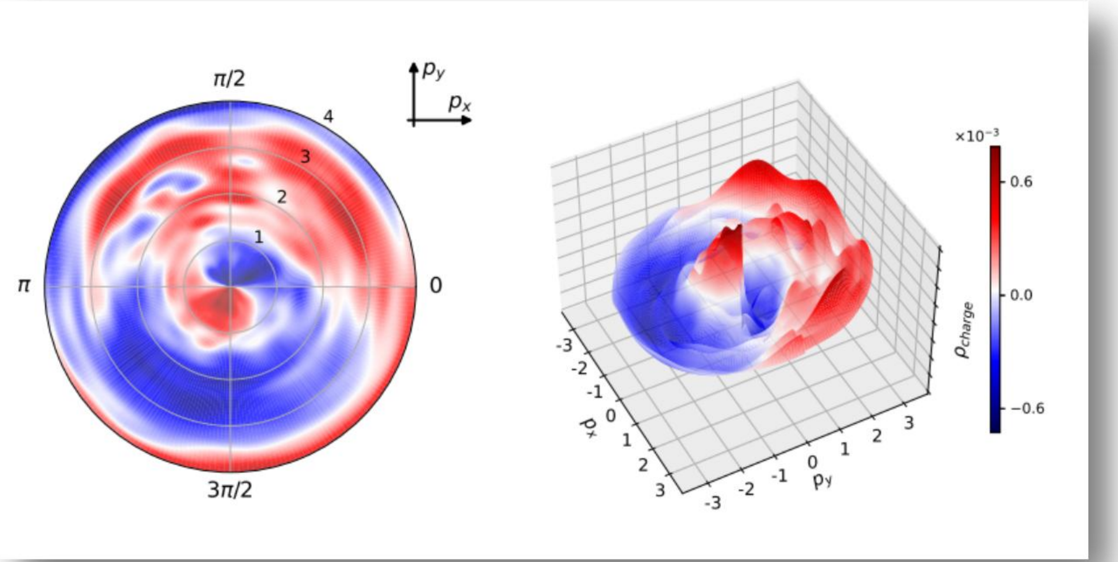

Gradient ascent to get the most responsive CME-spectra that demonstrates what has been learned by the machine.

YS.~Zhao, LWang, K.Zhou and XG.Huang,PRC 106 (2022) 5, L051901
SGuo, L.Wang, K.Zhou and G.L.Ma,RIKEN-iTHEMS-Report-25

Capture Short and Long range correlations

Dynamical Edge Convolution Network

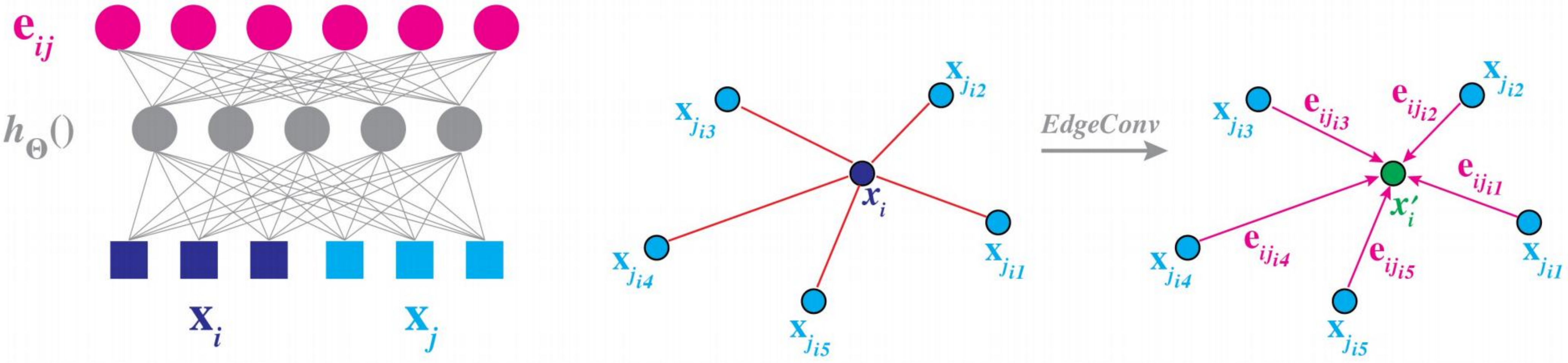

Fig. 2. **Left**: Computing an edge feature, $\mathbf{e}_{ij}$ (top), from a point pair, $\mathbf{x}_i$ and $\mathbf{x}_j$ (bottom). In this example, $h_\Theta()$ is instantiated using a fully connected layer, and the learnable parameters are its associated weights. **Right**: The EdgeConv operation. The output of EdgeConv is calculated by aggregating the edge features associated with all the edges emanating from each connected vertex.

Looking for self similarity in momentum space

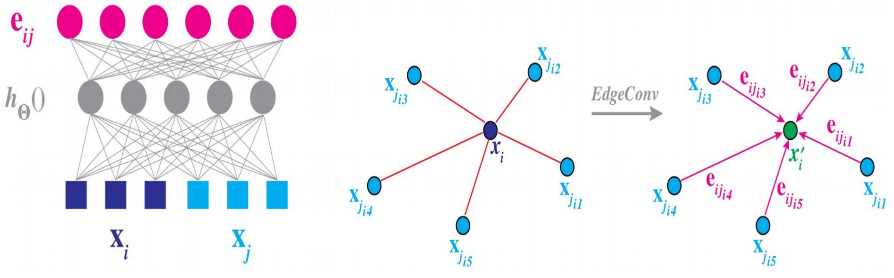

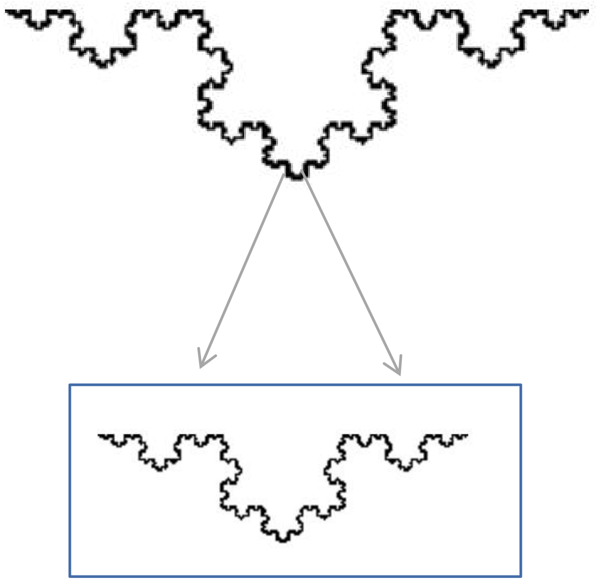

Self similarity, scaling invariance

Look for short-range and long-range correlations

Dynamical Edge Convolution Network

Tagging

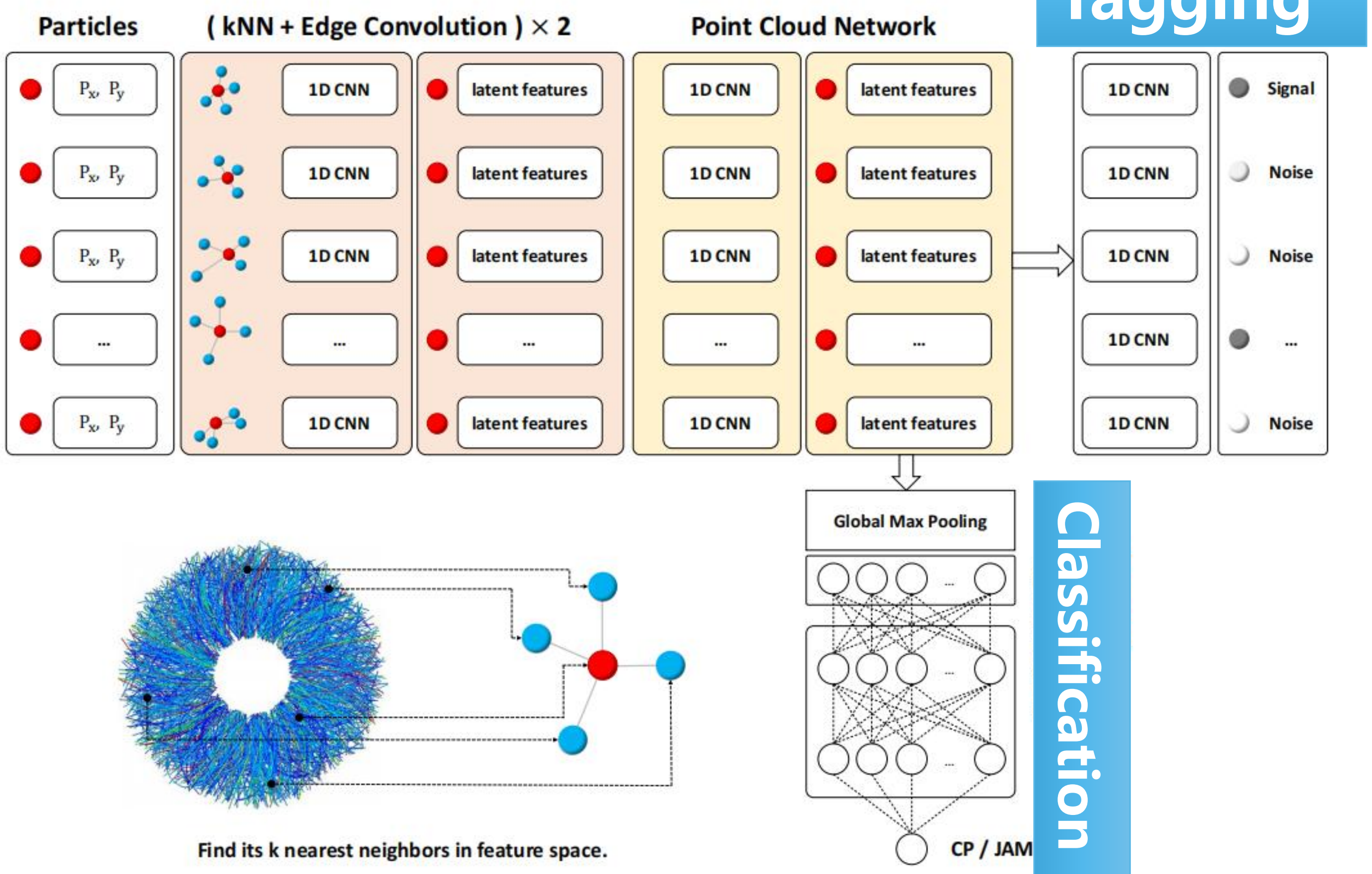

Classification

PLB 827(2022) 137001, Y.-G. Huang, L.-G. Pang, X.F. Luo and X.-N. Wang

Topological Data Analysis for CEP

Identifying weak critical fluctuations of intermittency in heavy-ion collisions with topological machine learning

Rui Wang,[1] Chengrui Qiu,[1] Chuan-Shen Hu,[2] Zhiming Li,[1,3,*] and Yuanfang Wu[1]

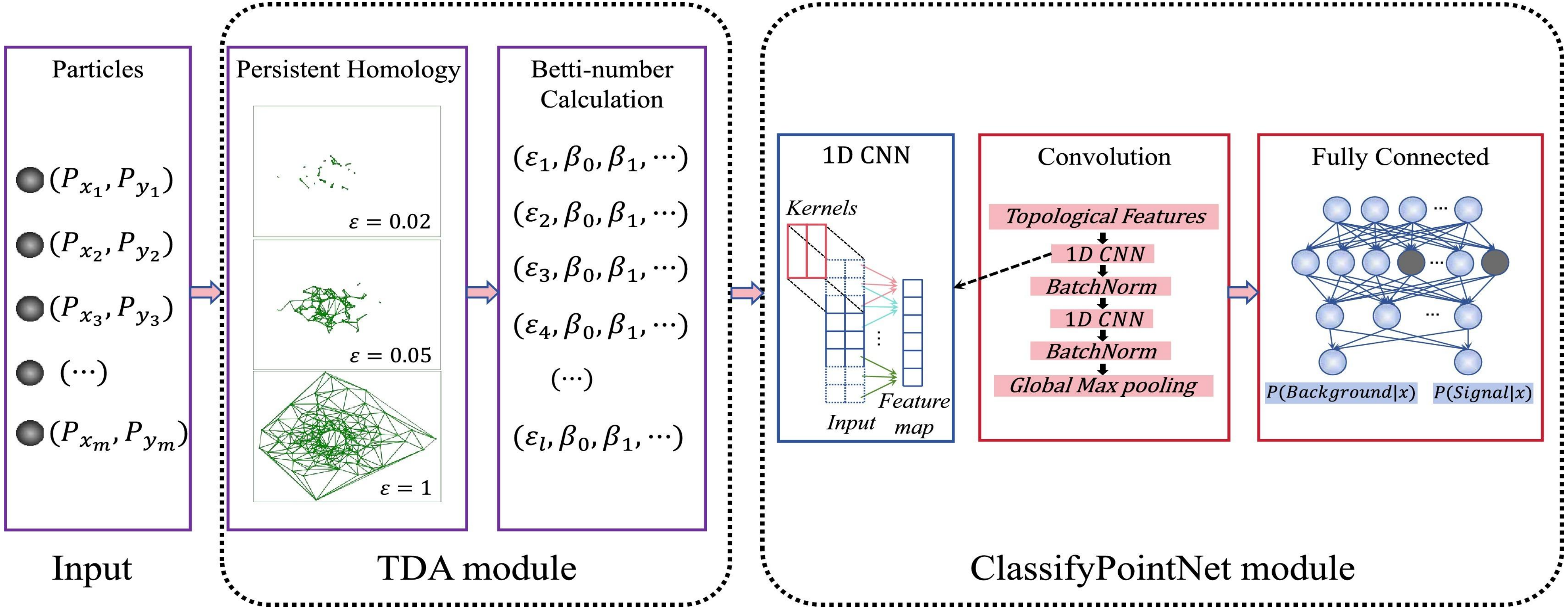

Phys.Lett.B 864 (2025) 139405

Critical endpoint from holographic QCD

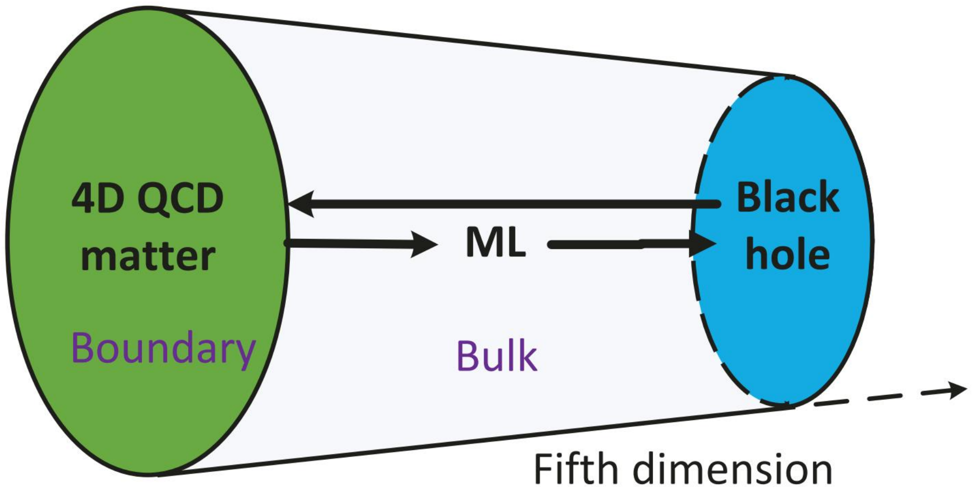

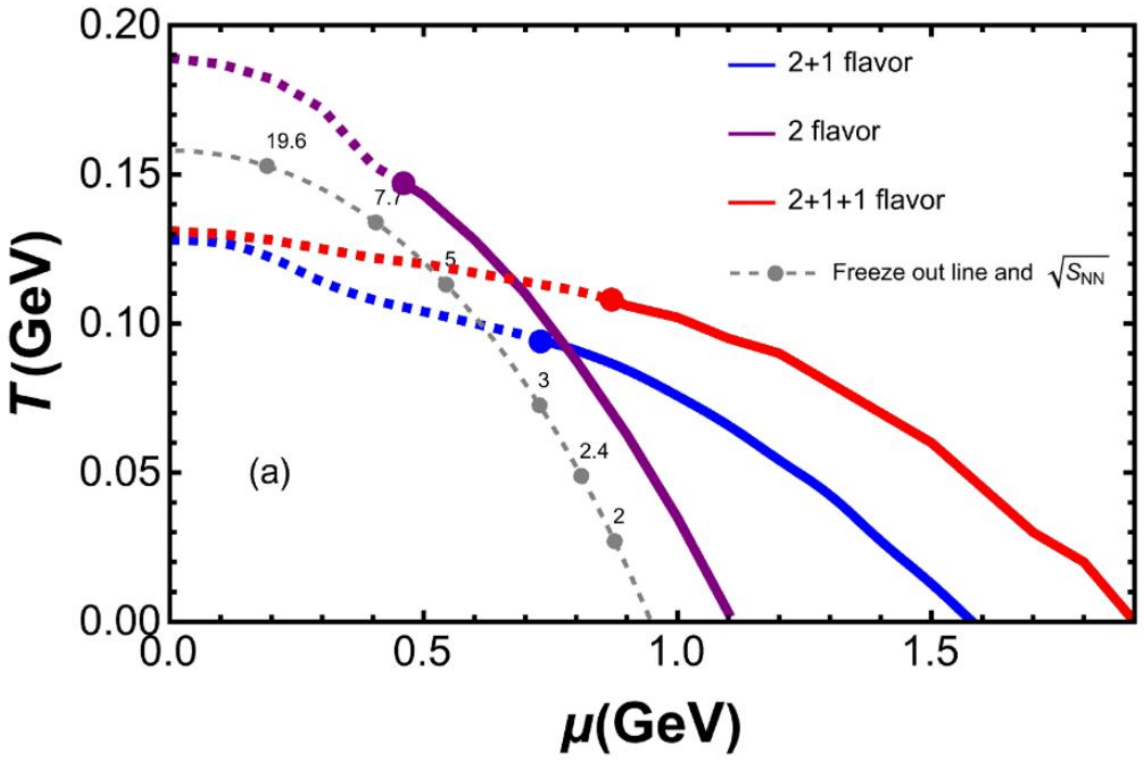

Einstein-Maxwell-Dilaton Framework with 6 parameters, determined by Lattice QCD at muB=0

Xun Chen, Mei Huang, JHEP 2025

Bayesian inference location of CEP

PHYS. REV. D 112, 026019 (2025)

Bayesian inference of the critical end point in a (2 + 1)-flavor system from holographic QCD

Liqiang Zhu,[1,*] Xun Chen,[1,2,3,†] Kai Zhou,[4,5,‡] Hanzhong Zhang,[1,§] and Mei Huang[6,‖]

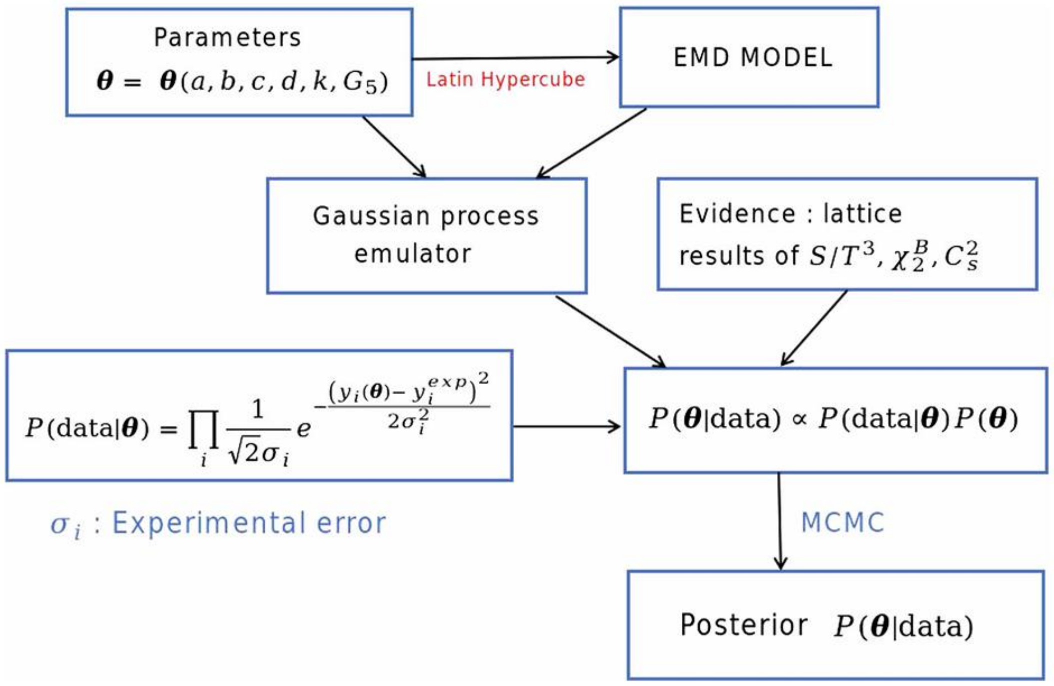

FIG. 1. Overview of the Bayesian parameter inference process.

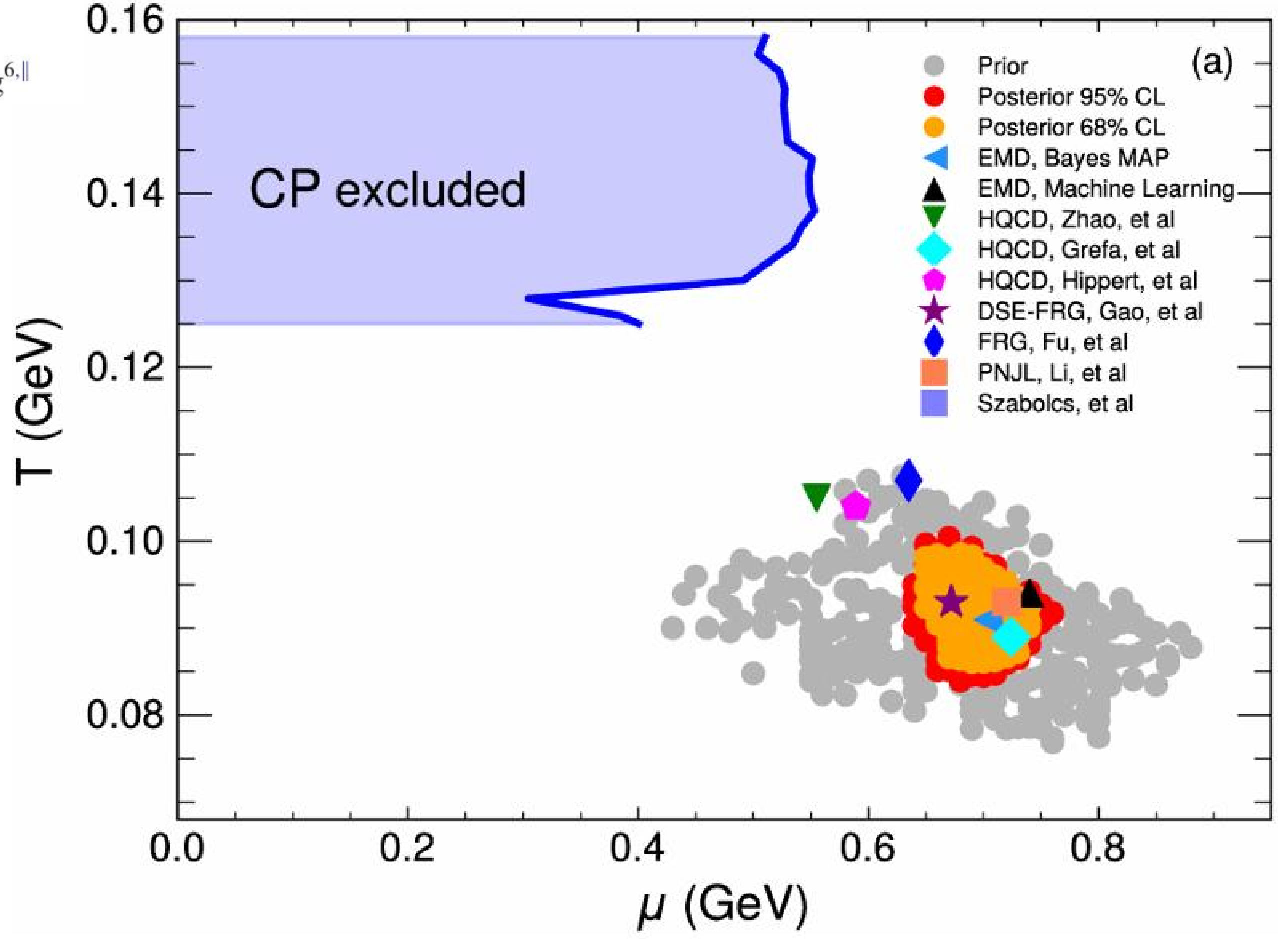

03

AutoDiff and PINNs

By embedding physical constraints into neural network architectures,PINNs have unique advantages in describing complex physical systems

Methods: Auto differentiation, Physics Informed Neural Network, Physically constrained

Variational Functions: Heavy quark potential in medium, M(T) of quasi partons, metric in AdS/CFT,

PDEs: dynamical evolutions, relativistic hydro, Transport Equations

Auto Differentiation: machine precision

Forward Mode

Introduce dual numbers: $x \to x + \dot{x}\mathbf{d}$

where $\mathbf{d}^2 = 0$

$$(x + \dot{x}\mathbf{d}) + (y + \dot{y}\mathbf{d}) = x + y + (\dot{x} + \dot{y})\mathbf{d}$$
$$(x + \dot{x}\mathbf{d}) - (y + \dot{y}\mathbf{d}) = x - y + (\dot{x} - \dot{y})\mathbf{d}$$
$$(x + \dot{x}\mathbf{d}) * (y + \dot{y}\mathbf{d}) = xy + (x\dot{y} + \dot{x}y)\mathbf{d}$$
$$\frac{1}{x + \dot{x}\mathbf{d}} = \frac{1}{x} - \frac{\dot{x}}{x^2}\mathbf{d} \qquad (x \neq 0)$$

Forward mode for $R^1 \to R^n$

Reverse mode for $R^n \to R^1$

Reverse Mode

adjoint number: $\bar{w} = \dfrac{\partial l}{\partial w}$

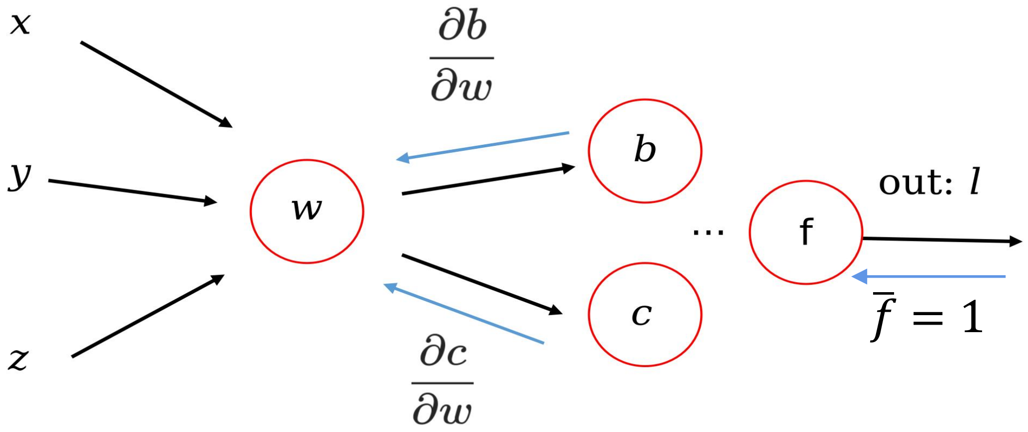

$$\text{step } 1: \bar{w} = 0$$
$$\text{step } 2: \bar{w} = \bar{w} + \bar{b}\frac{\partial b}{\partial w}$$
$$\text{step } 3: \bar{w} = \bar{w} + \bar{c}\frac{\partial c}{\partial w}$$

Differential Program，Physics Informed Neural Network

Training Neural Network

Coil Optimization via AutoDiff

$$B(r) = \sum_{i=1}^{N_c} \sum_{n=1}^{N_1} \sum_{b=1}^{N_2} \frac{\mu_0 I_{n,b}^i}{4\pi} \oint \frac{dl_{n,b}^i \times (r - r_{n,b}^i)}{|r - r_{n,b}^i|^3}.$$

coil parameters

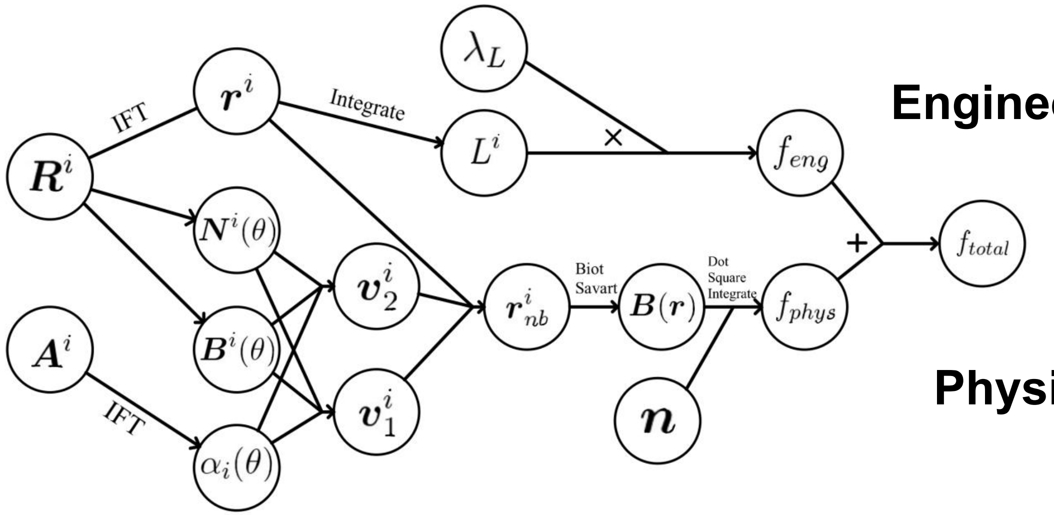

Engineering obj.

Physical obj.

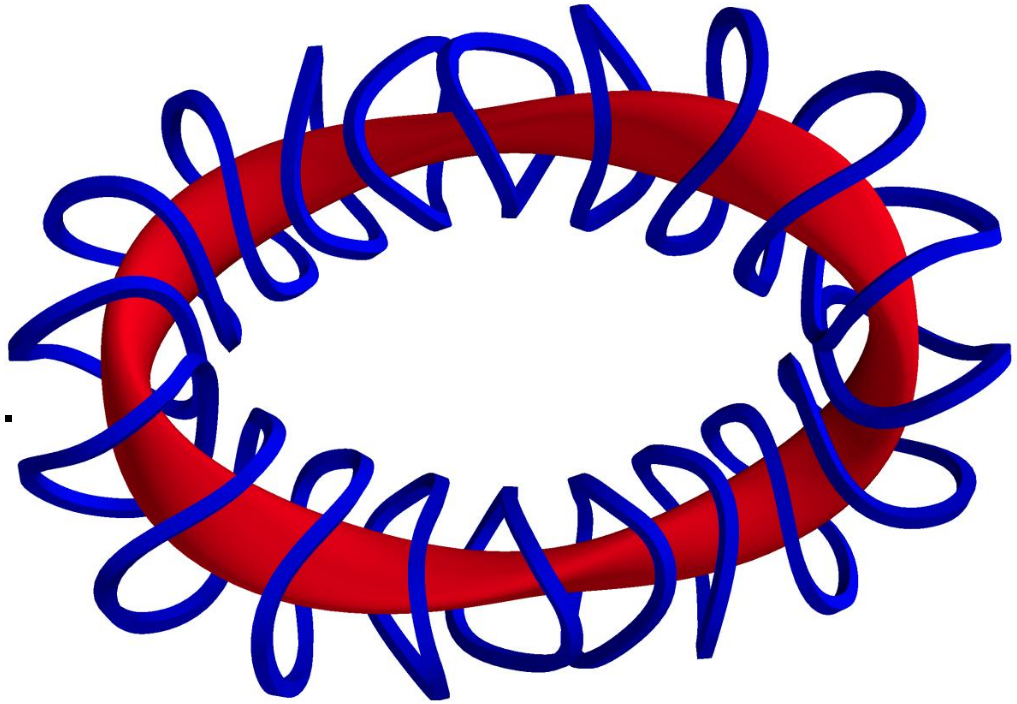

N McGreivy N, SR Hudson , CX Zhu. 2020, arXiv:2009.00196

Objective: Magnetic confinement of plasma via engineered coils.
Workflow: R, A → IFT → Integration → Biot-Savart Law → B(r)
Optimization Targets: (1) **Engineering**: Minimize total coil length.
(2) **Physics**: Ensure **B** is tangent (parallel) to the plasma boundary.

Blue coils & **red plasma**

In medium heavy quark potential

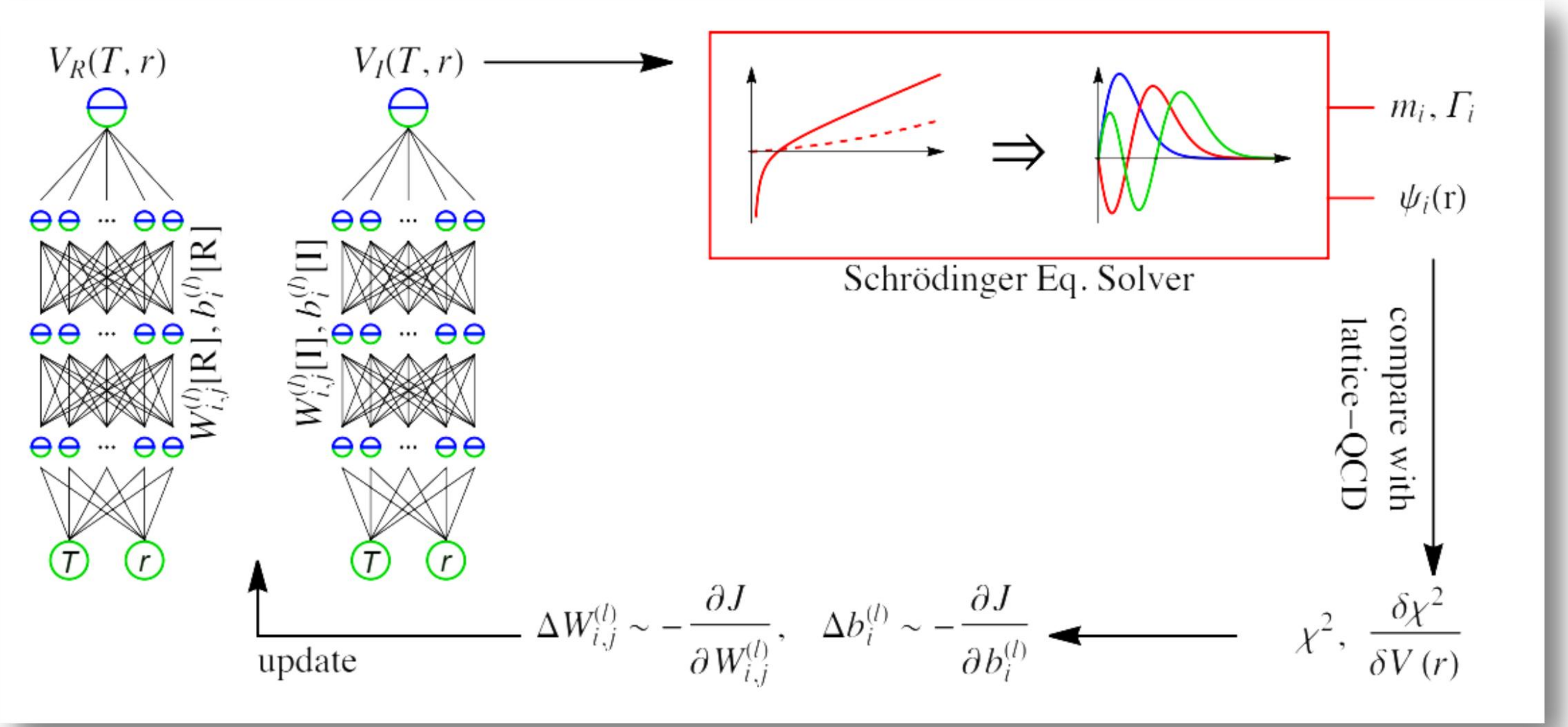

S.Z. Shi, K. Zhou, J.X. Zhao, S. Mukherjee, and P.F. Zhuang Phys. Rev. D 105, 014017

Deep Learning Quasi Parton Model

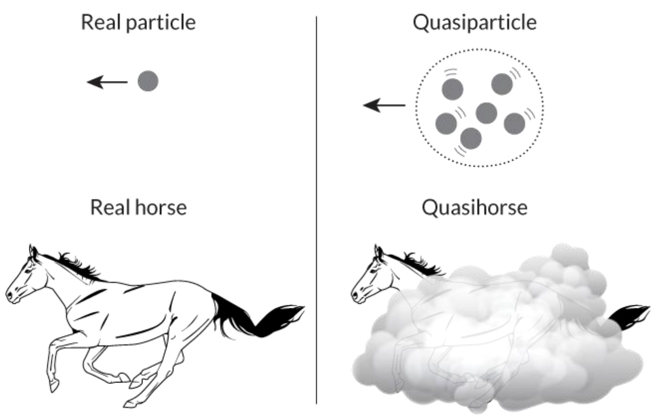

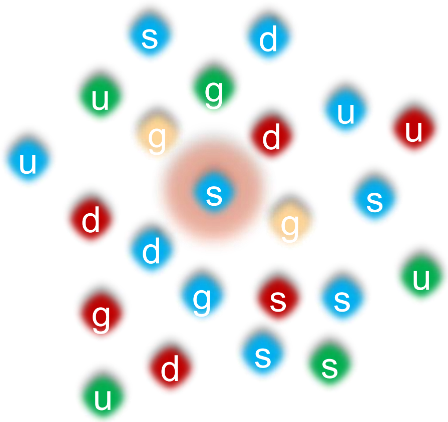

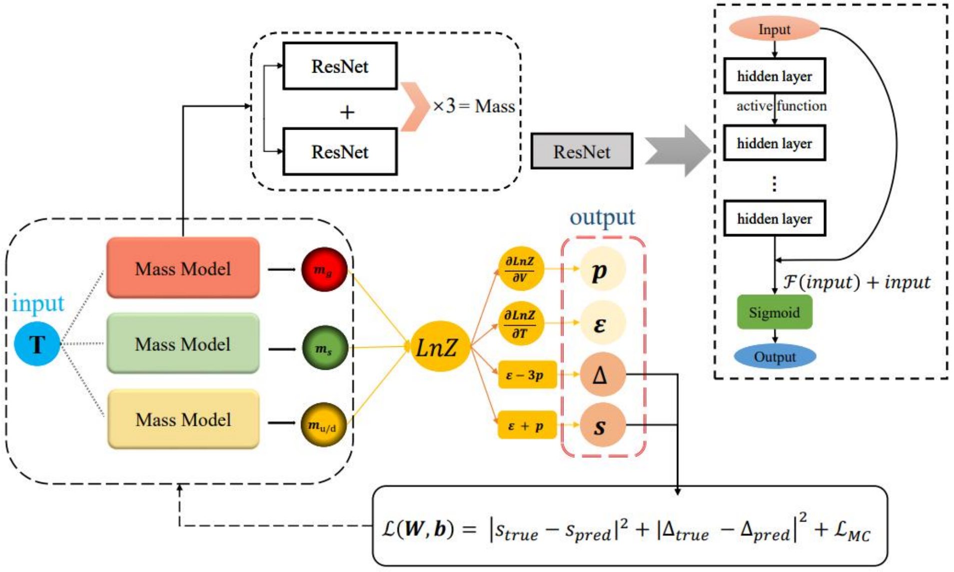

$$\ln Z(T) = \ln Z_g(T) + \ln Z_{u,d}(T) + \ln Z_s(T),$$

Fermi-Dirac distributions,

$$\ln Z_g(T) = -\frac{16V}{2\pi^2}\int_0^\infty p^2 dp \ln\left[1 - \exp\left(-\frac{1}{T}\sqrt{p^2 + m_g^2(T)}\right)\right], \quad (2)$$

$$\ln Z_{q_i}(T) = +\frac{12V}{2\pi^2}\int_0^\infty p^2 dp \ln\left[1 + \exp\left(-\frac{1}{T}\sqrt{p^2 + m_{q_i}^2(T)}\right)\right], \quad (3)$$

quarks, $m_s(T, \theta_2)$ for strange quark and $m_g(T, \theta_3)$ for gluons, where θ_1, θ_2 and θ_3 are the parameters in DNN shown in Fig. 1.

The resulting pressure and energy density are computed using the following statistical formulae,

$$P(T) = T\left(\frac{\partial \ln Z(T)}{\partial V}\right)_T, \quad (5)$$

$$\epsilon(T) = \frac{T^2}{V}\left(\frac{\partial \ln Z(T)}{\partial T}\right)_V, \quad (6)$$

Consistent QCD EoS and eta/s

EoS vs Lattice QCD

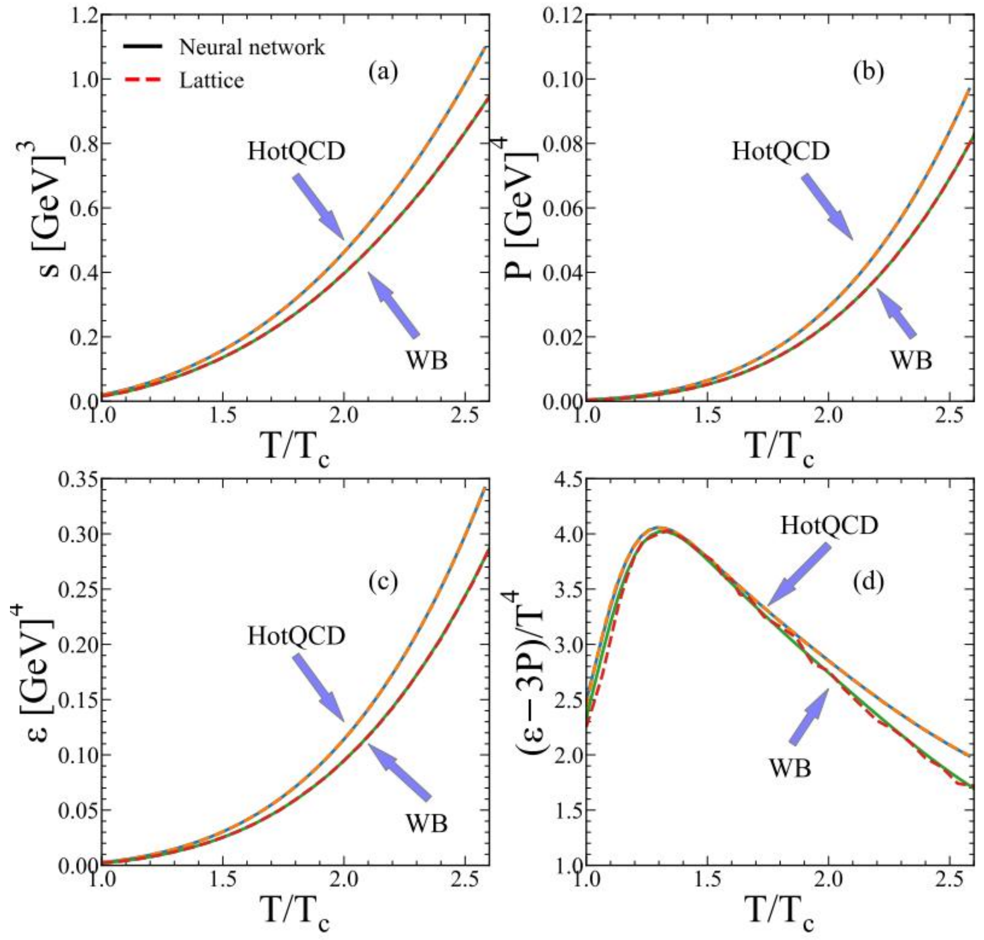

Learned Mass

η/s

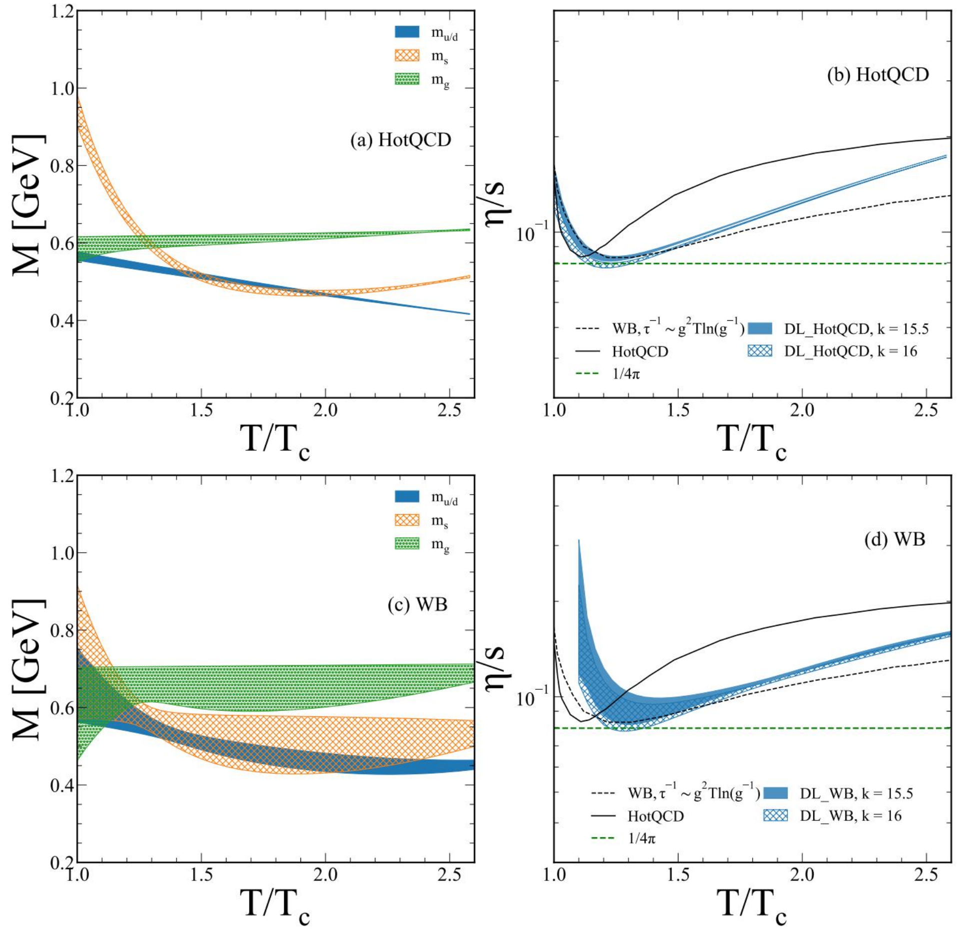

FuPeng Li, HL Lu, LG Pang, GY Qin, PLB 2023

2D Quasi Parton Model: $\boldsymbol{m(T, \mu_B)}$

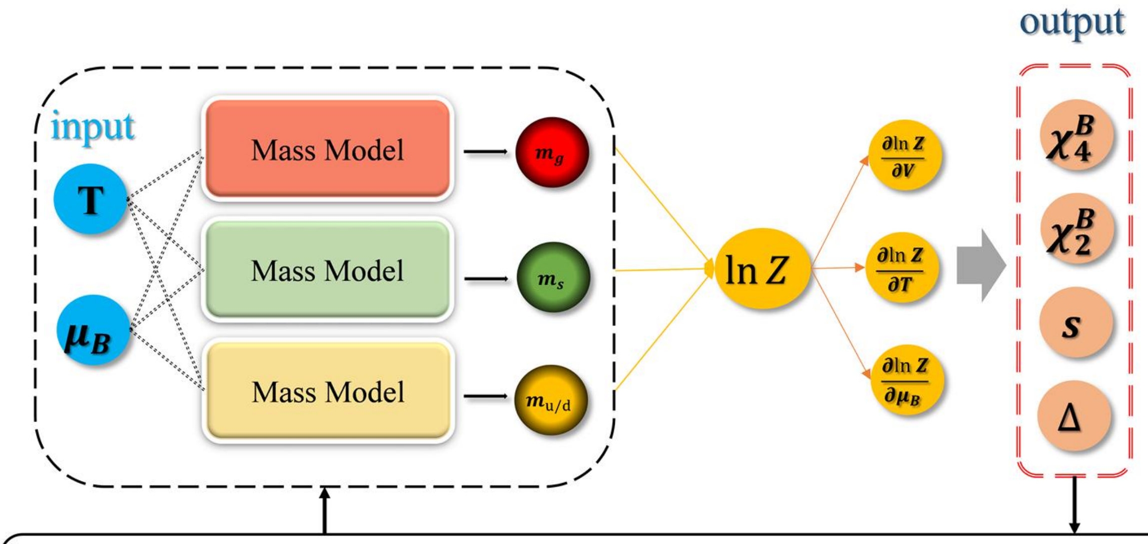

$$\mathcal{L}(\theta_1, \theta_2, \theta_3) = |s_{NN} - s_{input}| + |\frac{|\Delta\ _{NN} - \Delta\ _{input}}{T}| + |\chi^B_{2,NN} - \chi^B_{2,input}| + |\chi^B_{4,NN} \text{ - } \chi^B_{4,input}| + \mathcal{L}_{MC}$$

Equation Of State

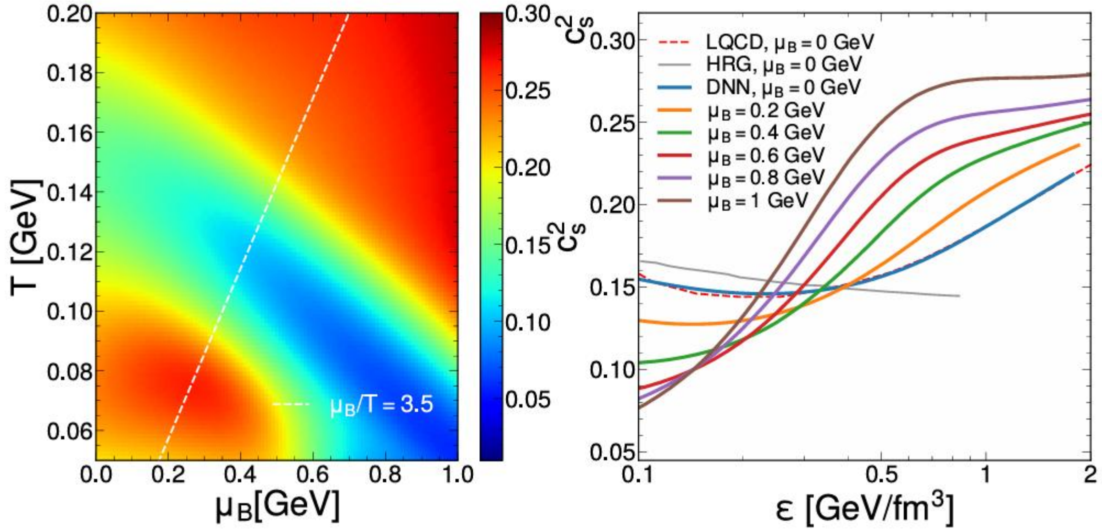

FP Li, LG Pang, GY Qin. PLB 868 (2025) 139692

4D Quasi Parton Model: $\boldsymbol{m}(\boldsymbol{T}, \boldsymbol{\mu_B}, \boldsymbol{\mu_Q}, \boldsymbol{\mu_S})$

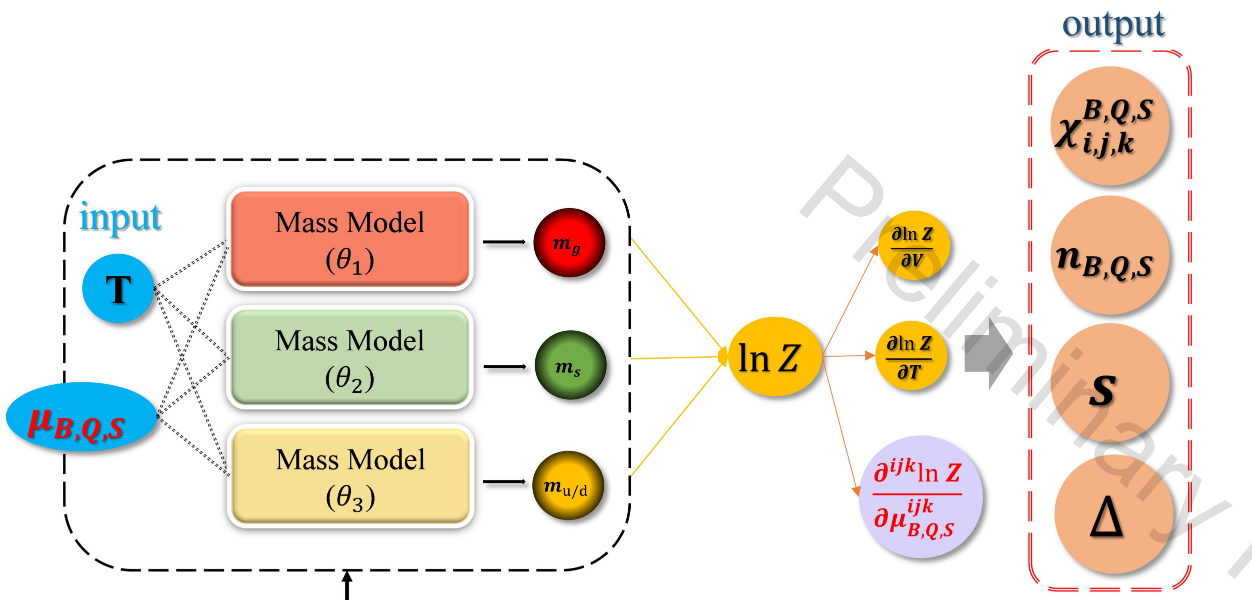

$$\mathcal{L}(\theta_1, \theta_2, \theta_3) = |s_{DNN} - s_{LQCD}| + |\frac{|\Delta_{DNN} - \Delta_{LQCD}}{T}| + |\chi^{B,Q,S}_{i,j,k,DNN} - \chi^{B,Q,S}_{i,j,k,LQCD}| + |n_{B,Q,S}| + | + \mathcal{L}_{MC}$$

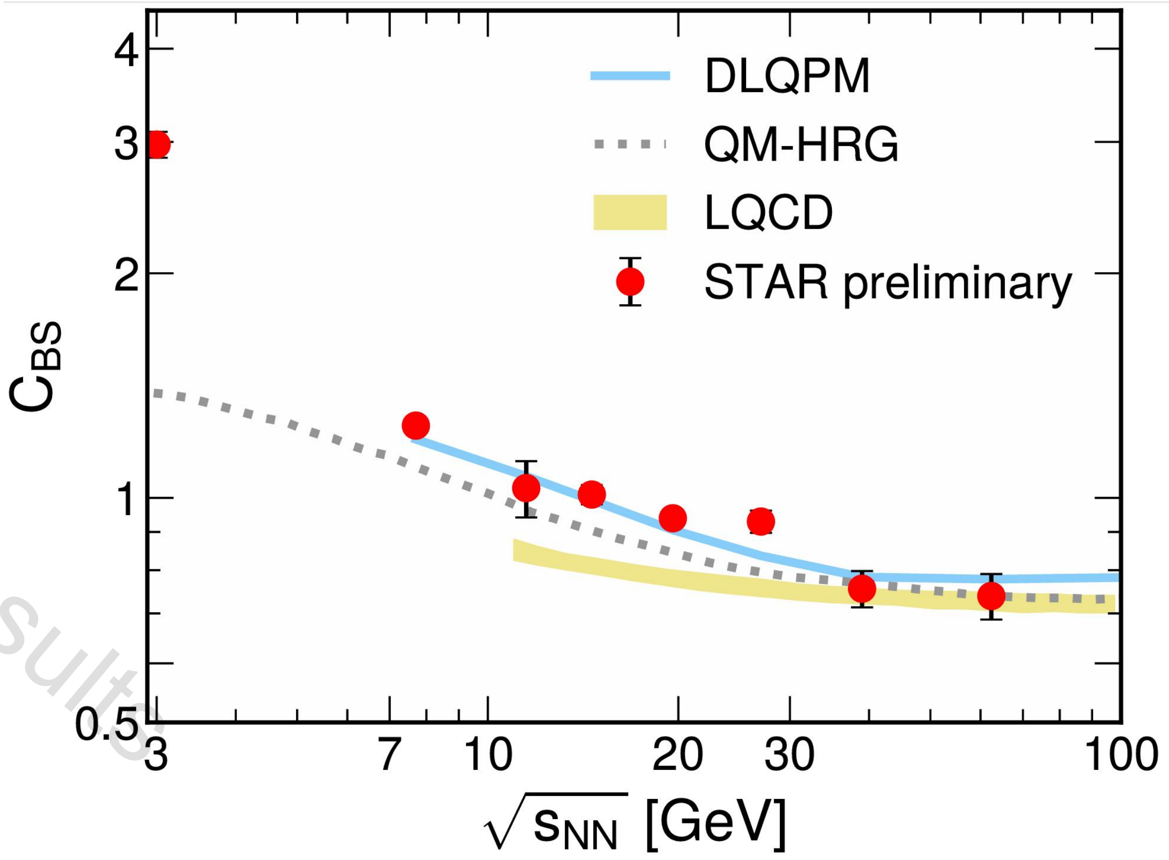

FP Li, LG Pang, GY Qin. in prepare

Auto-Diff for parton fragmentation function

$$\frac{\partial}{\partial \ln Q^2} D_i^{h^\pm}(x,Q) = \frac{\alpha_s(Q)}{2\pi} P_{ij}(x,\alpha_s) \otimes D_j^{h^\pm}(x,Q)$$

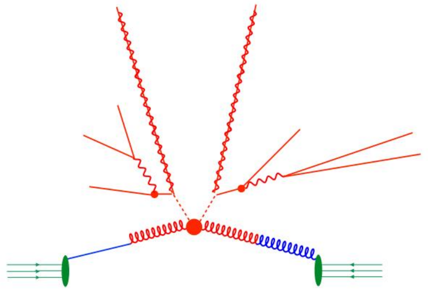

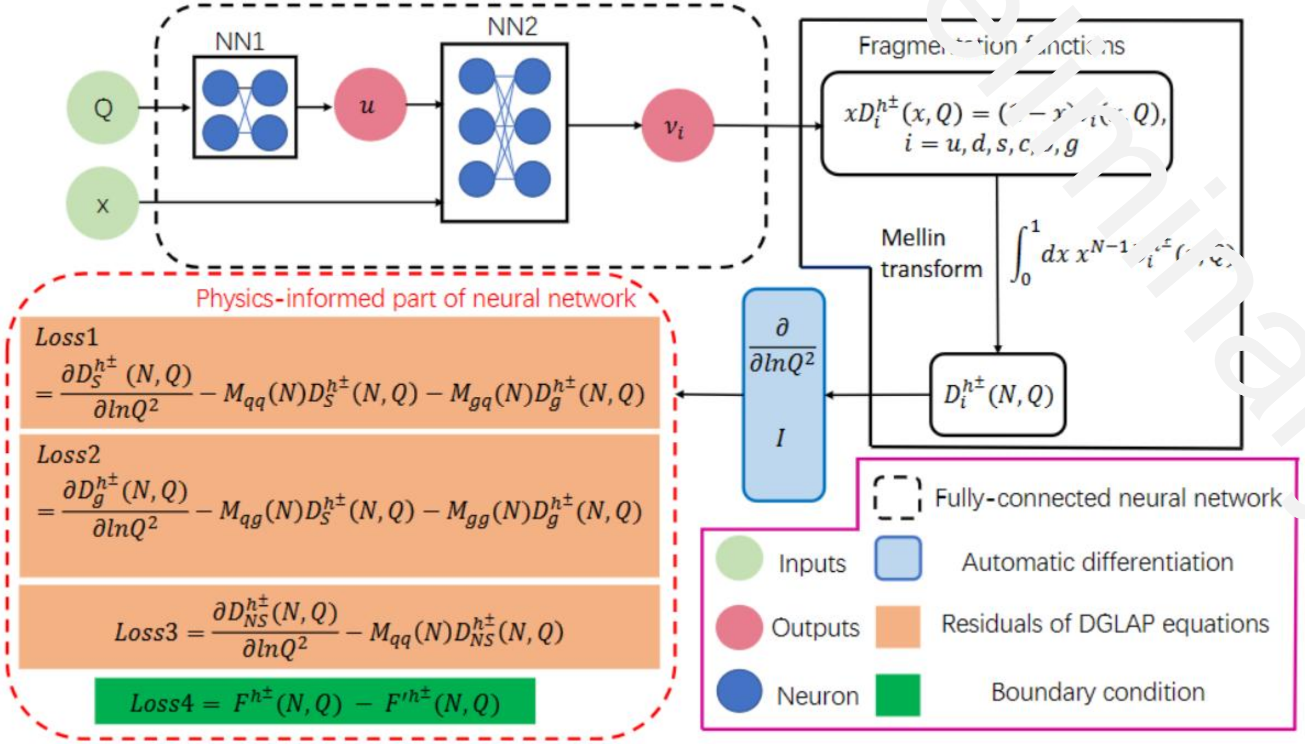

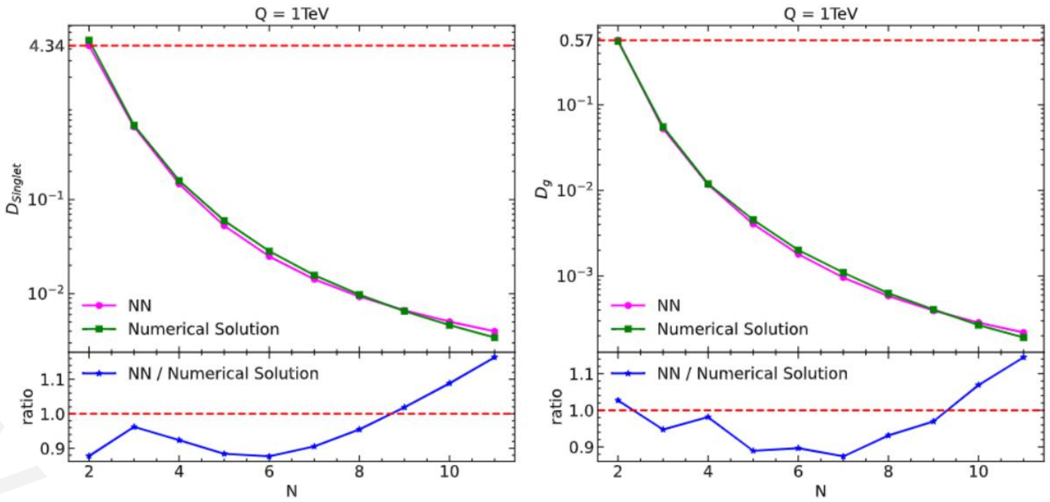

Preliminary

1. The results agree with traditional method
2. Automatic satisfies DGLAP evolution

SW Dai, FP Li, LG Pang, XN Wang, BW Zhang, HZ Zhang, in prepare

Exploring hadron–hadron interactions

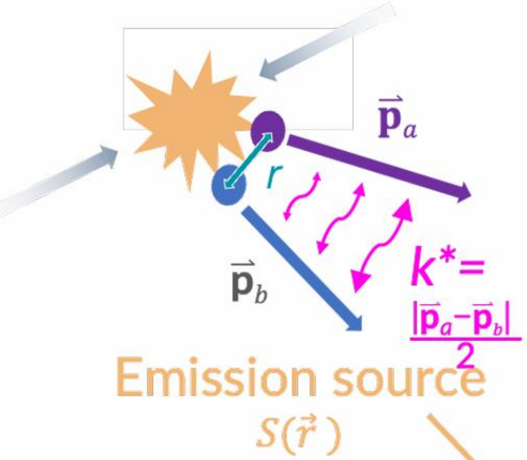

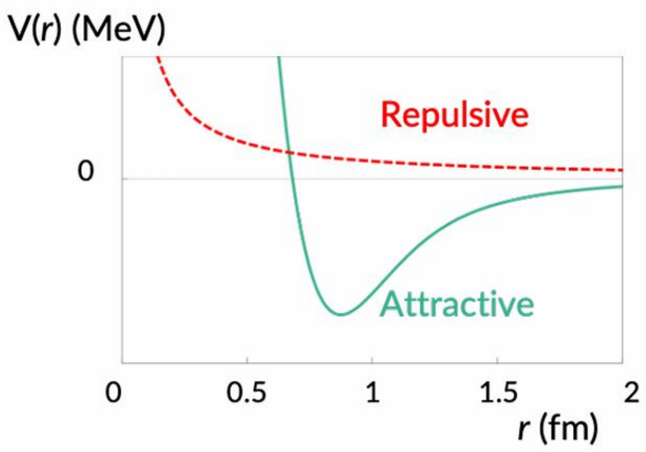

?

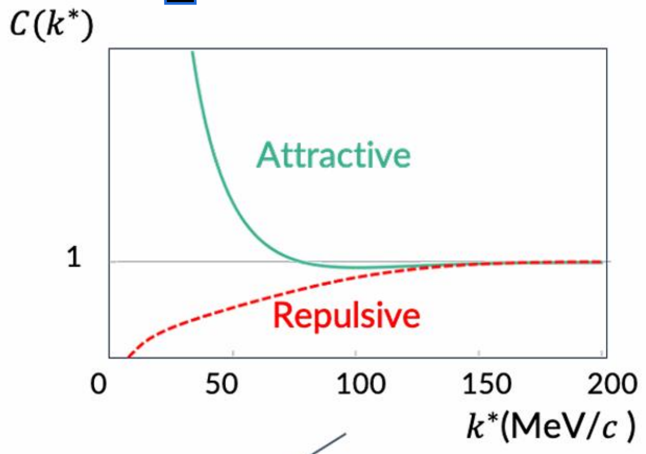

Correlations

Scattering Length
Effective Range

Two-particle wave function

$$C(k^*) = \int \overbrace{S(\vec{r})}\,\overbrace{|\psi(\vec{k}^*,\vec{r})|^2}\, d^3\vec{r} = \overbrace{\mathcal{N}(k^*)\frac{N_{\mathrm{same}}(k^*)}{N_{\mathrm{mixed}}(k^*)}}$$

Raffaele Del Grande | XQCD 2023

Lednicky-Lyuboshits(LL) analytic model
(Asymptotic wave-function+
Effective range correlation+
Gaussian source)

Lednicky, Lyuboshits, Sov.J.Nucl.Phys. 35 (1982) 770

DL for emission sorce

Learning Hadron Emitting Sources with Deep Neural Networks

Lingxiao Wang[1] and Jiaxing Zhao[2,3,*]

$$C(k) = \int S(\boldsymbol{r})|\psi_k(\boldsymbol{r})|^2 d\boldsymbol{r},$$

Traditional：Gaussian Source

$$S(r) = \frac{1}{(4\pi r_0^2)^{3/2}} \exp\left(-\frac{r^2}{4r_0^2}\right).$$

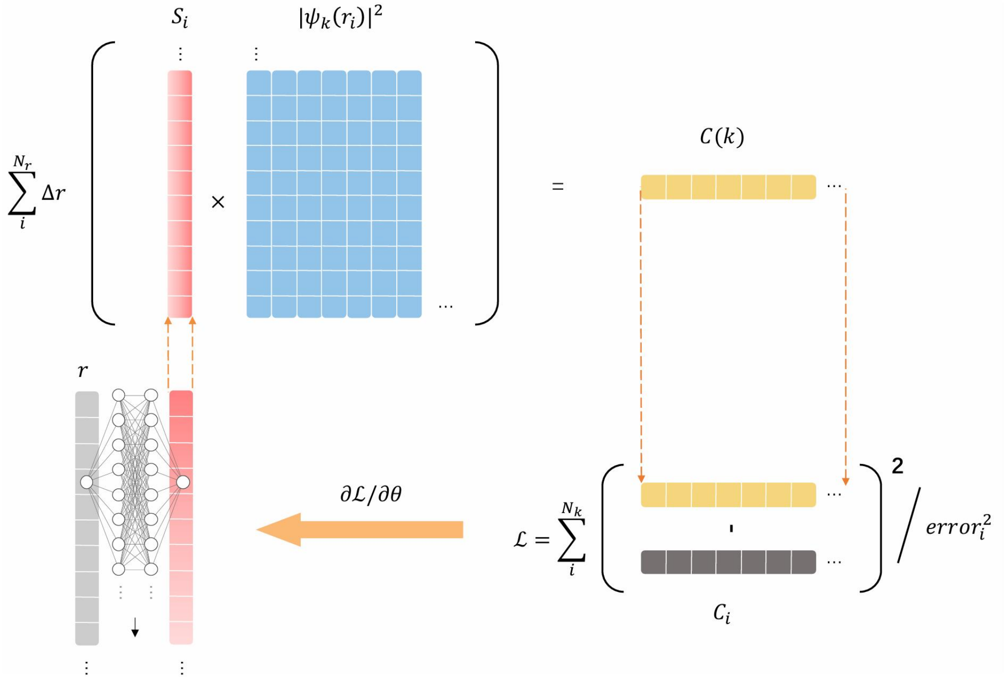

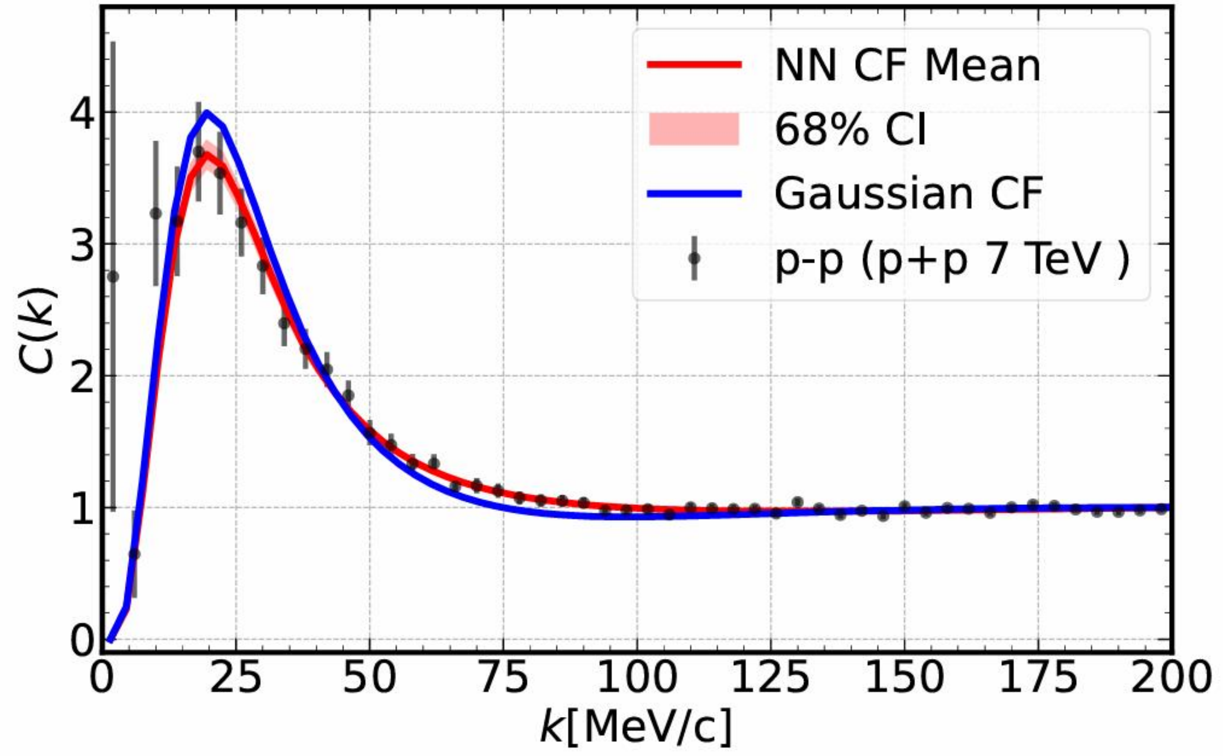

NN：Neural Network Source

02

Generative Models

Providing data-driven event generation methods for heavy-ion collision, with the potential to replace or supplement traditional first-principles simulators

Methods: VAE, GAN, flow model, diffusion model, flow matching, transformer

Applications: Fast simulations of HICs, Geant, Hydro, UrQMD, Parton transport models

Benifit: Millions of times speed up

Generativive models： MC sampling

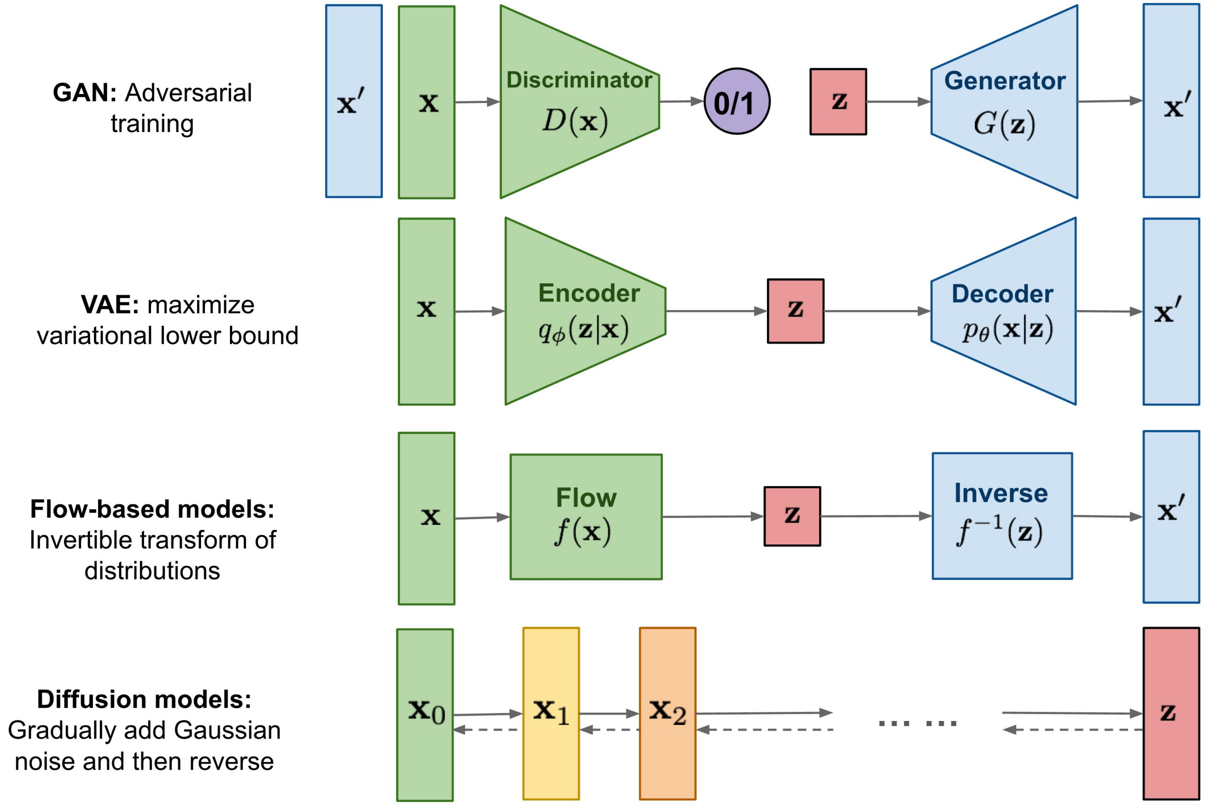

Similar to Box Muller algorithm

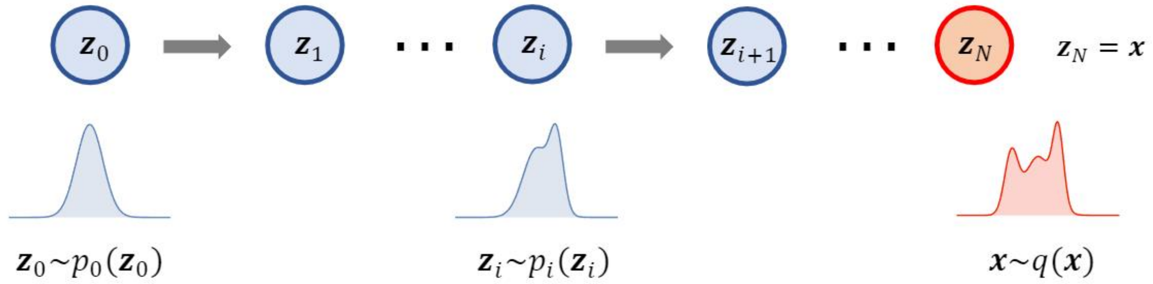

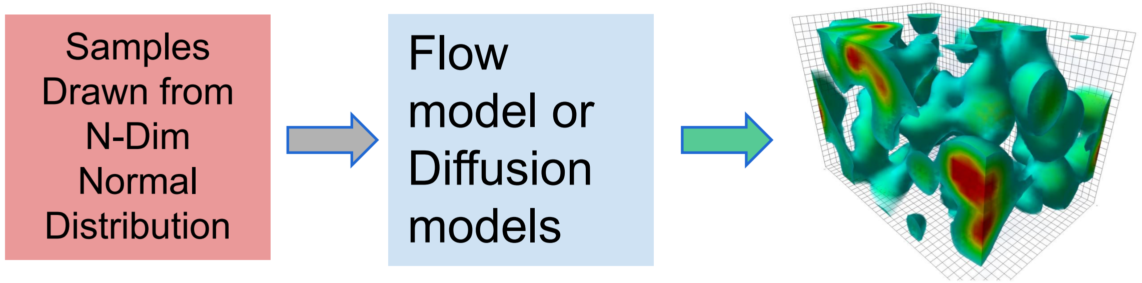

Flow-based generative models for Markov chain Monte Carlo in lattice field theory
Albergo, Kanwar, Shanahan 1904.1207

Diffusion model for HIC simulations

An end-to-end generative diffusion model for heavy-ion collisions

arXiv:2410.13069

Jing-An Sun,[1,2] Li Yan,[1,3] Charles Gale,[2] and Sangyong Jeon[2]

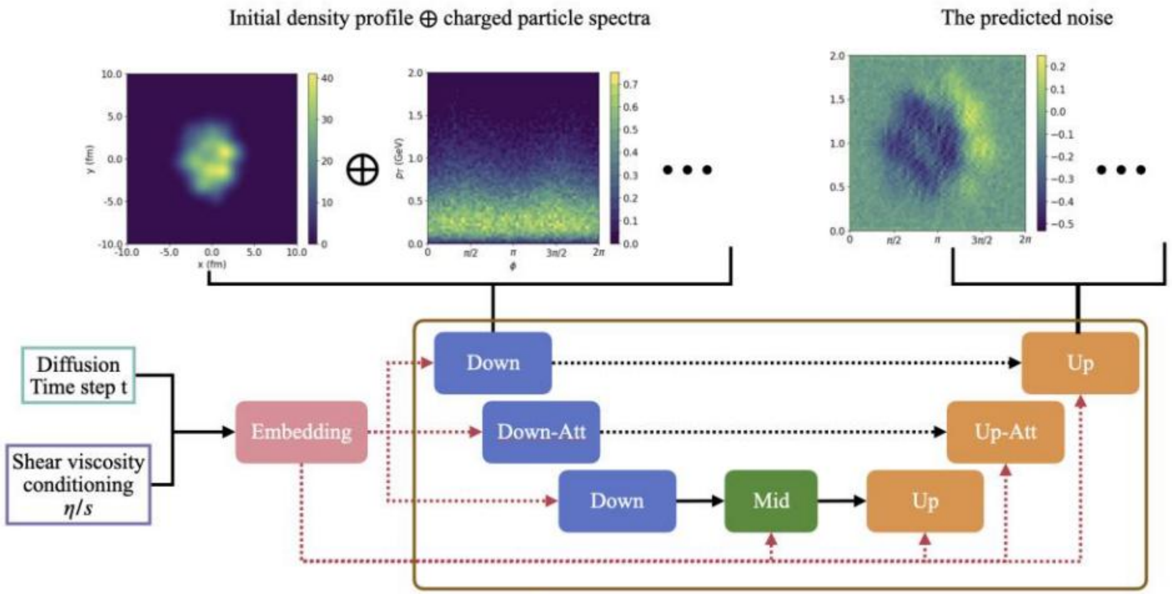

$$\boldsymbol{S}_t = \sqrt{\bar{\alpha}_t}\boldsymbol{S}_0 + \sqrt{1-\bar{\alpha}_t}\boldsymbol{\varepsilon}$$

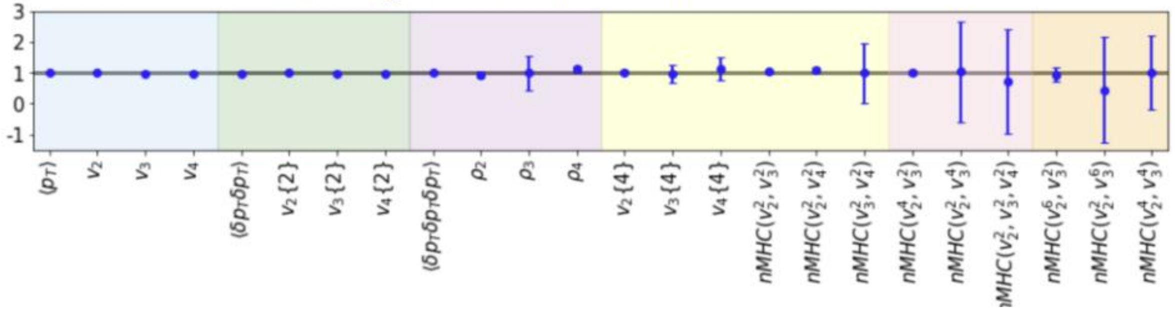

tor. We carried out (2+1)D minimum bias simulations of Pb-Pb collisions at 5.02 TeV, choosing the shear viscosity η/s to be one of three distinct values: 0.0, 0.1, and 0.2. For each value of η/s, we generate 12,000 pairs of initial entropy density profiles and final particle spectra, corresponding to 12,000 simulated events, as the training dataset. 70% of the total events are used for training and the rest are used for validation.

Considering that the spectra $\boldsymbol{S}_0$ depend on the initial entropy density profiles $\boldsymbol{I}$ and the shear viscosity η/s, we train a conditional reverse diffusion process $p(\boldsymbol{S}_0|\boldsymbol{I}, \eta/s)$ without modifying the forward process.

one single central collision event in just 10^{-1} seconds on a GeForce GTX 4090 GPU.

ble precision, as the traditional numerical simulation of hydrodynamics for one central event typically takes approximately 120 minutes (10^4 seconds) on a single CPU.

Generative model for HICs

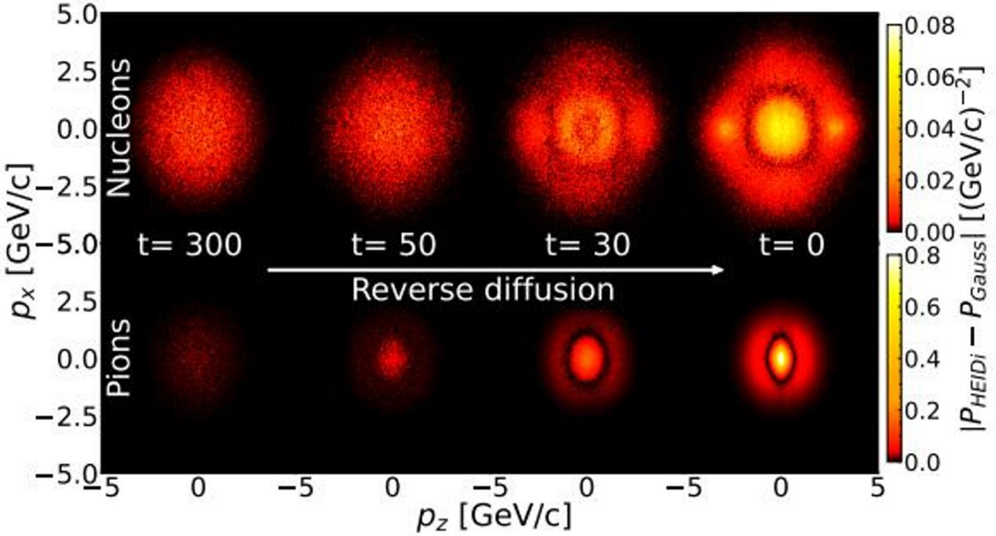

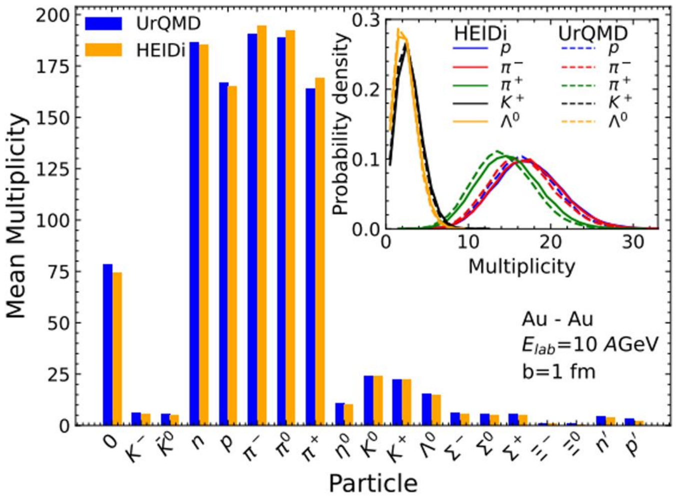

M. O.K, K. Z, J. S, H. S, arXiv: 2502.16330, arXiv:2412.10352

18k **UrQMD** simulation events for training

HEIDi:
Heavy-ion Events through Intelligent Diffusion

PointNet encoder +
Normalizing flow decoder +
Pointcloud diffusion

credit: https://lilianweng.github.io/

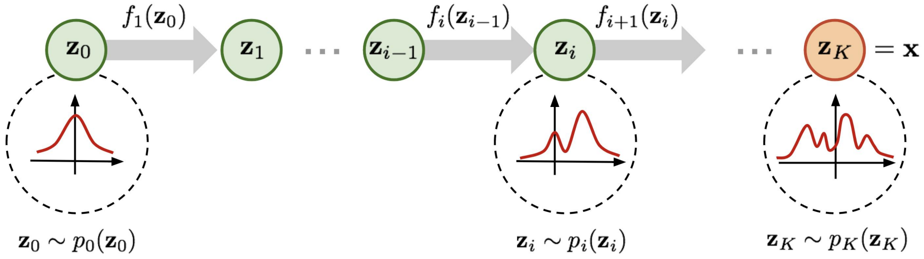

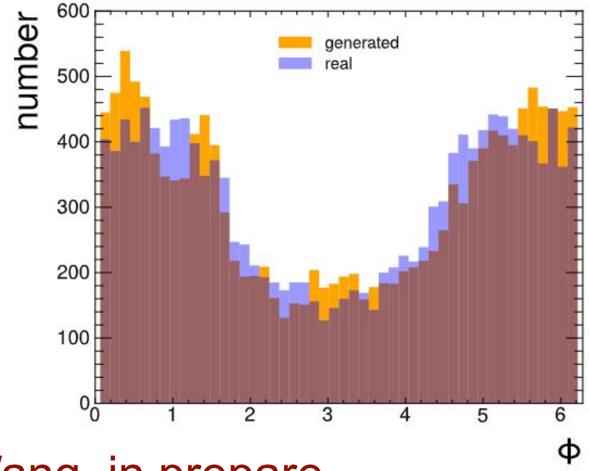

K.Y. Wu, Z. Yang, L.G. Pang and X.N. Wang, in prepare

Event-by-event jet eloss and medium response

Flow model and flow matching are used to learn the high dimensional distribution for faster medium response sampler

Stacked U-net for relativistic hydro

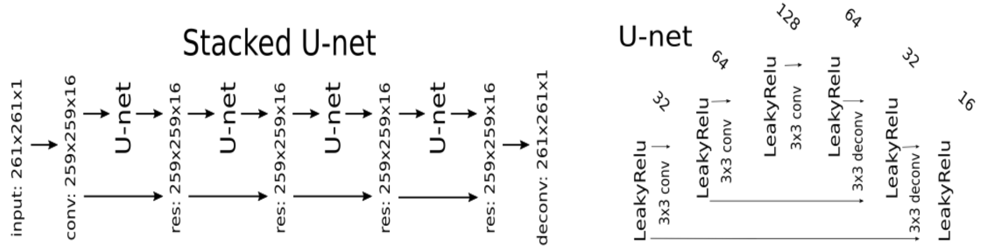

FIG. 1: An illustration of the encode-decode network, **stacked U-net**, which consists of the input and out layers and four residual U-net blocks. The right figure shows the U-net structure, and the depth of the hidden layer is written on the top of them.

The expansion of quark gluon plasma is learned in the image translation task using stacked UNET.

$$\nabla_\mu T^{\mu\nu} = 0$$

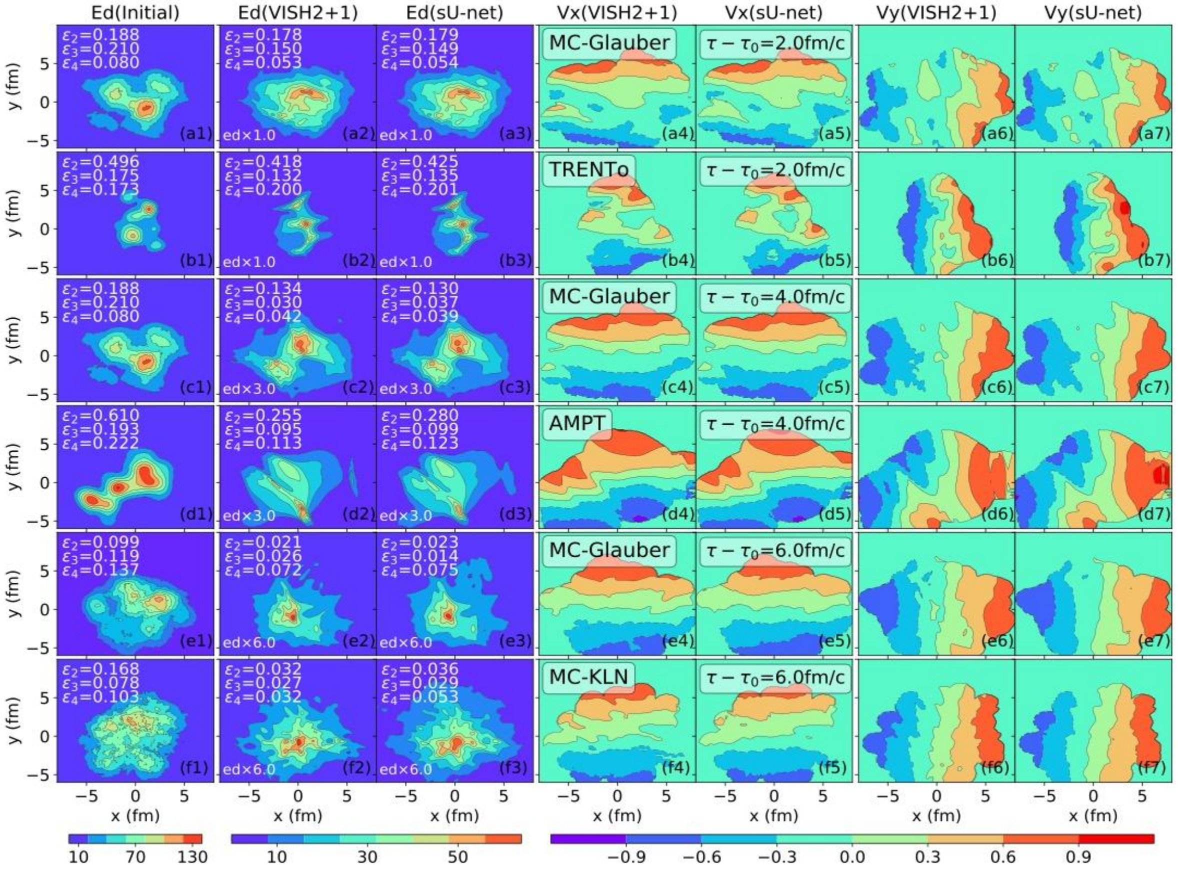

arXiv: 1801.03334; NPA2018, H.Huang, B.Xiao, H.Xiong, Z.Wu, Y. Mu and H.Song

04

Other Applications

Including unsupervised learning、Bayesian analysis、active learning and RL methods, providing new approaches and tools for heavy-ion collision research

Unsupervised Learning:
PCA, T-SNE, VAE,
Contrastive learning

Bayesian analysis:
precise physics,
uncertainty estimations

Active learning:
data efficent, small
labeled data

More
RL, Bayesian
Optimization

05

Challenges and Outlook

Model Dependence

Heavy reliance on the fidelity of physics models and effective theory.

Performance is bounded by the accuracy of the underlying assumptions.

Interpretability

The optimization process is often a "black box".

Lack of intuitive, physics-driven insight into why a specific configuration is optimal.

Generalization & Extrapolation

Solutions are often tailored to specific scenarios.

Uncertain reliability when applied to large muB regions (without constrains from data).

05

Challenges and **Outlook**

Outlook: The Autonomous AI HEP-Physicist

An LLM-powered agent that reasons like a human physicist, formulating hypotheses and designing numerical/physical experiments

Deep, Context-Aware Research

Automating the literature review cycle

Closed-Loop Scientific Discovery

Fully autonomous pipeline: from theoretical design and experimental planning to data analysis and the discovery of novel physics insights.

Review articles

Nature Review Physics (2025)

nature reviews physics https://doi.org/10.1038/s42254-024-00798-x

Perspective Check for updates

Physics-driven learning for inverse problems in quantum chromodynamics

Gert Aarts[1], Kenji Fukushima[2], Tetsuo Hatsuda[3], Andreas Ipp[4], Shuzhe Shi[5], Lingxiao Wang[3] & Kai Zhou[6,7]

Abstract

The integration of deep learning techniques and physics-driven designs is reforming the way we address inverse problems, in which accurate physical properties are extracted from complex observations. This is particularly relevant for quantum chromodynamics (QCD) – the theory of strong interactions – with its inherent challenges in interpreting

Sections

Introduction

Physics-driven learning

QCD physics

Conclusions and outlook

Review Of Modern Physics (2022)

Colloquium: Machine learning in nuclear physics

Amber Boehnlein, Markus Diefenthaler, Nobuo Sato, Malachi Schram, Veronique Ziegler, Cristiano Morten Hjorth-Jensen, Tanja Horn, Michelle P. Kuchera, Dean Lee, Witold Nazarewicz, Peter Ostro Orginos, Alan Poon, Xin-Nian Wang, Alexander Scheinker, Michael S. Smith, and Long-Gang Pang

Rev. Mod. Phys. **94**, 031003 – Published 8 September 2022

Article | References | No Citing Articles | PDF | HTML | Export Citation

Prog. Part. Nucl. Phys. 135 (2024) 104084

Progress in Particle and Nuclear Physics 135 (2024) 104084

Contents lists available at ScienceDirect

Progress in Particle and Nuclear Physics

journal homepage: www.elsevier.com/locate/ppnp

ELSEVIER

Review

Exploring QCD matter in extreme conditions with Machine Learning

Kai Zhou[a,b,*], Lingxiao Wang[a,*], Long-Gang Pang[c,*], Shuzhe Shi[d,e,*]

[a] Frankfurt Institute for Advanced Studies (FIAS), D-60438 Frankfurt am Main, Germany
[b] School of Science and Engineering, The Chinese University of Hong Kong, Shenzhen 518172, China
[c] Institute of Particle Physics and Key Laboratory of Quark and Lepton Physics (MOE), Central China Normal University, Wuhan, 430079, China
[d] Department of Physics, Tsinghua University, Beijing 100084, China

Nuclear Science and Techniques (2023) 34:88
https://doi.org/10.1007/s41365-023-01233-z

REVIEW ARTICLE

Nucl. Sci. Tech. 34 (2023) 6, 88

High-energy nuclear physics meets machine learning

Wan-Bing He[1,2] · Yu-Gang Ma[1,2] · Long-Gang Pang[3] · Hui-Chao Song[4] · Kai Zhou[5]

: 18 April 2023 / Published online: 21 June 2023

Thank you!

Science China Physics, Mechanics & Astronomy

Machine learning in nuclear physics at low and intermediate energies

Wanbing He,[1,2,*] Qingfeng Li,[3,4,†] Yugang Ma,[1,2,‡] Zhongming Niu,[5,§] Junchen Pei,[6,7,¶] and Yingxun Zhang[8,9,**]

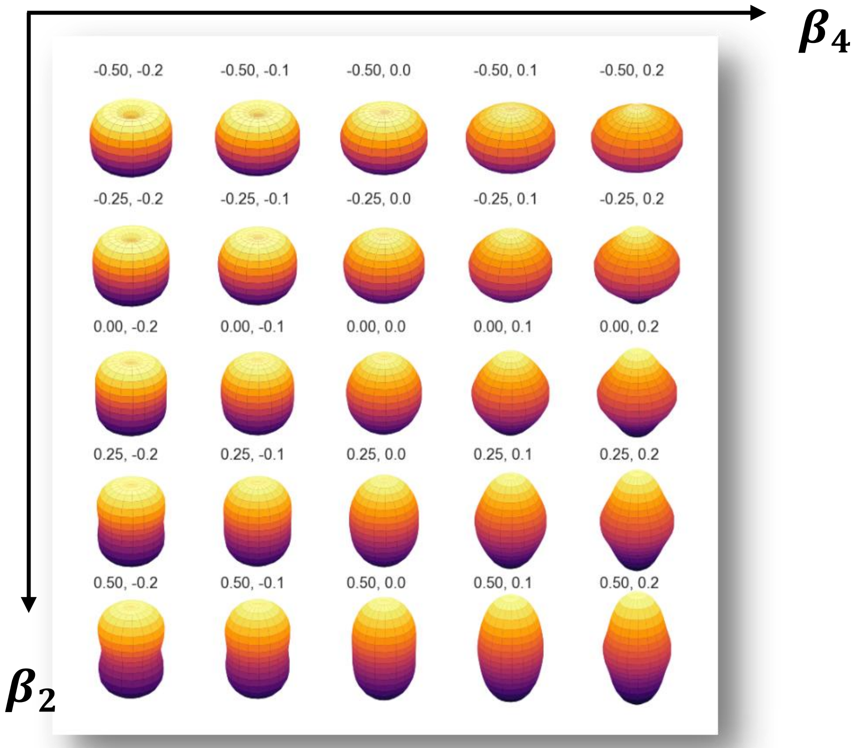

Data: Trento + Matching

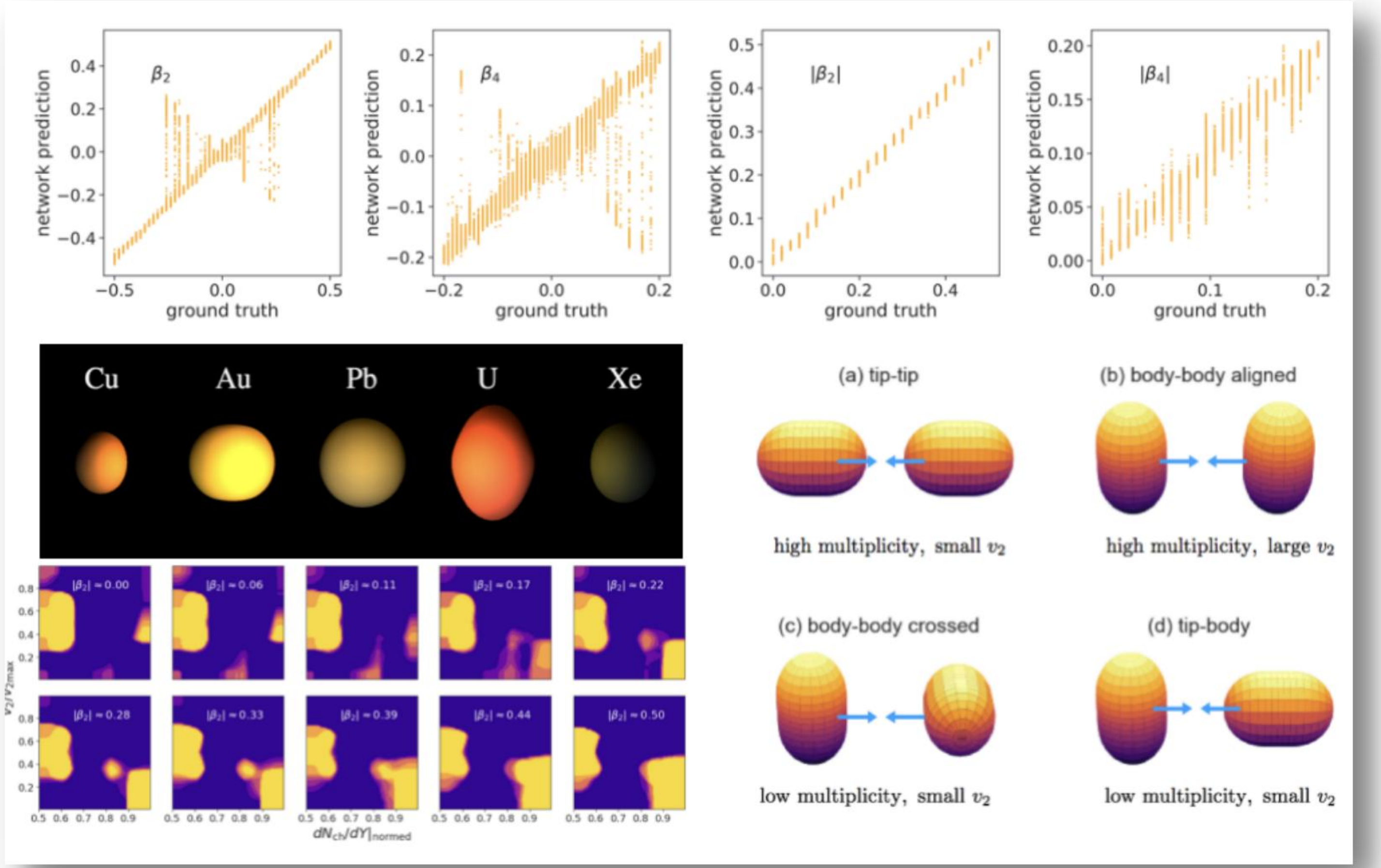

L.-G. Pang, K. Zhou and X.-N. Wang, arXiv:1906.06429

Identifying the α-clustering structure

α clusters | Fail in EbE | Succeed with 4000-events average

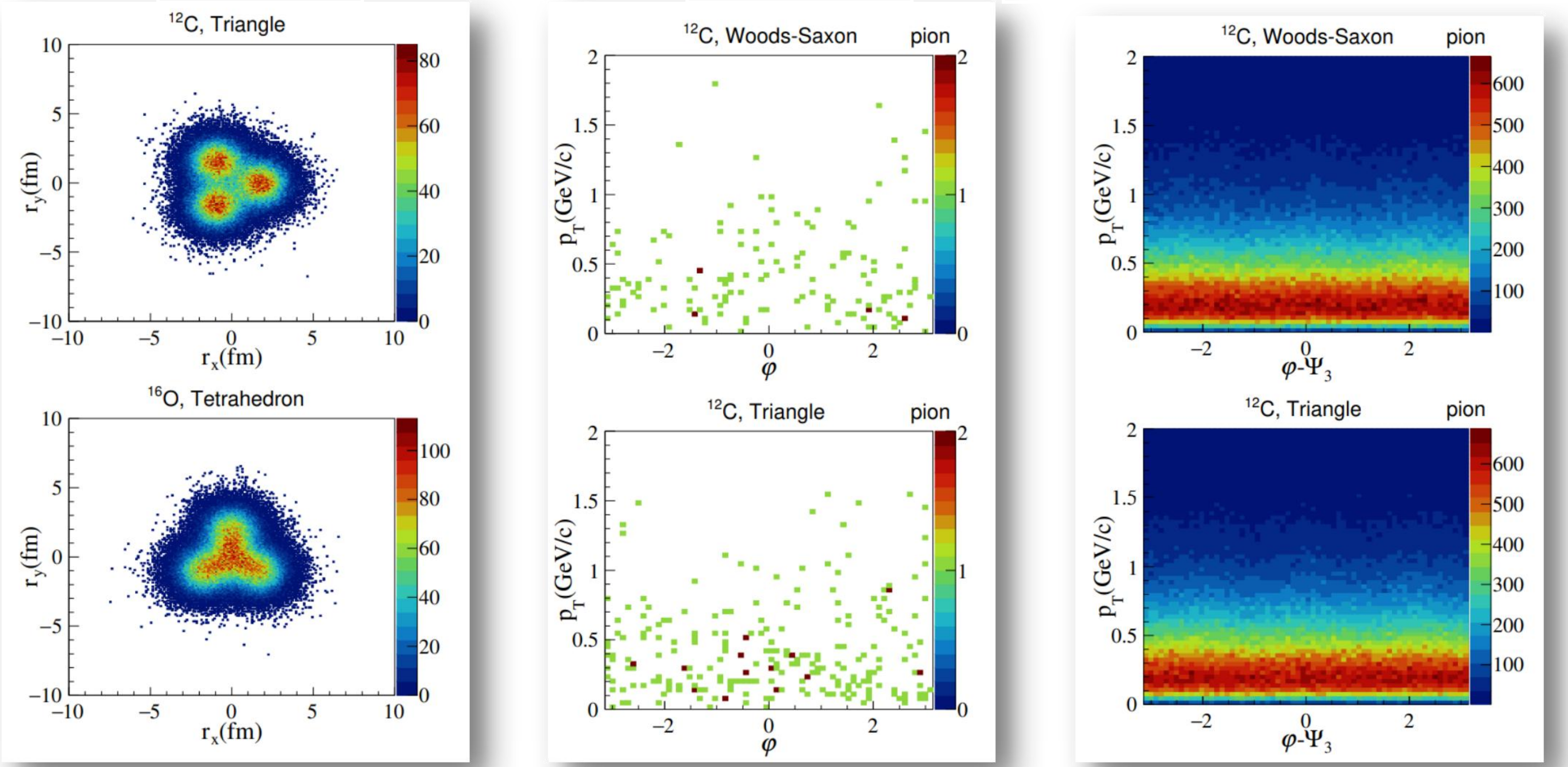

Junjie He, Wan-Bing He, Yu-Gang Ma, Song Zhang PRC 104, 044902 (2021)

Nucleon nucleon SRC

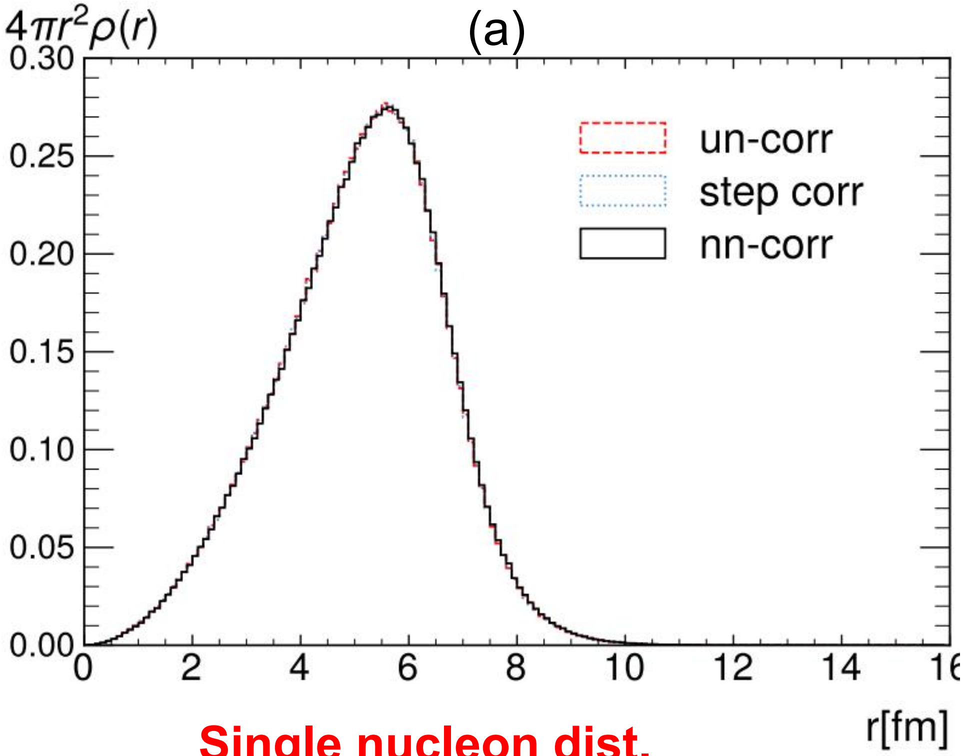

Single nucleon dist.

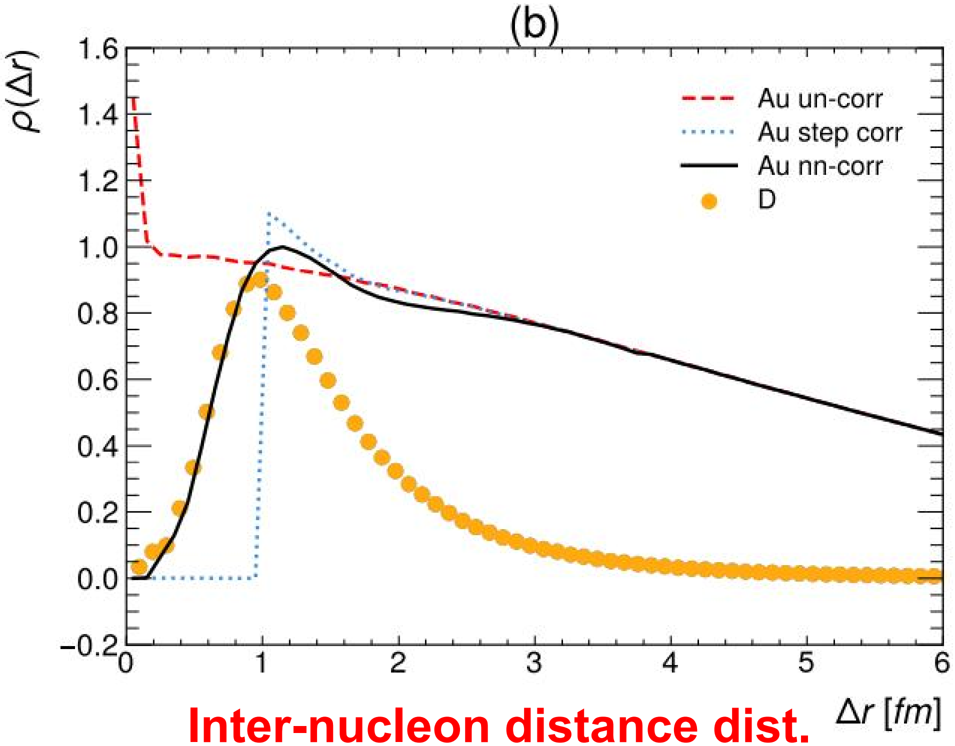

Inter-nucleon distance dist.

We developped a Monte carlo method to sample nucleons in Au nucleus obeying not only the single nucleon distribution $\rho(r)$ but also the two-nucleon distribution $\rho(\Delta r)$

Y.J. Huang, Z. Meng, L.G. Pang, X.N. Wang, arXiv:2504.00790

A novel neural network for nn correlations

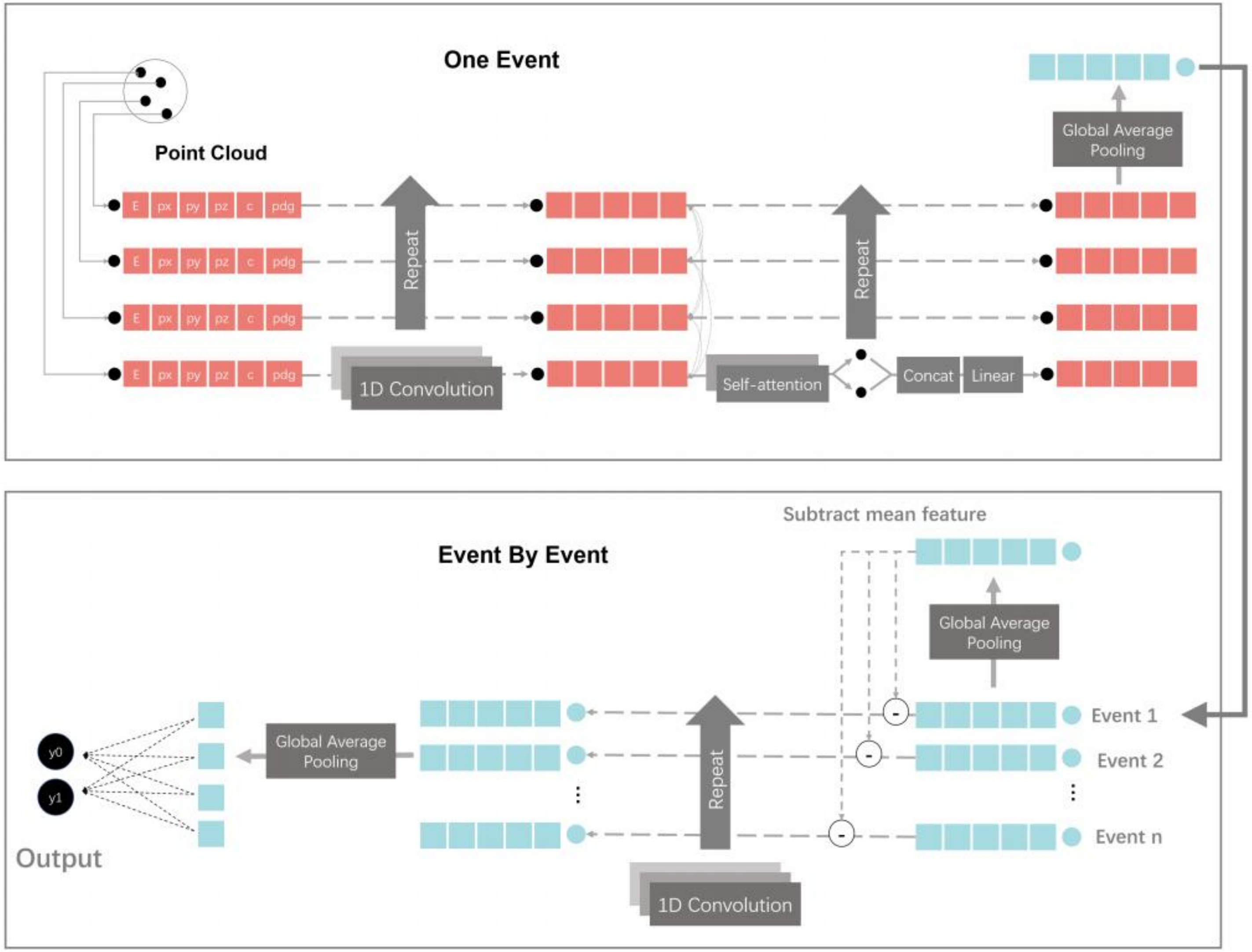

Network structure

- Point cloud network
- Self attention (used in large language models like chatgpt and deepseek)
- Multi-event mixing

Correlations of latent features

$$\overline{f(z_1 - \bar{z}_1, z_2 - \bar{z}_2, \cdots, z_n - \bar{z}_n)}$$

where z_i is the i-th latent feature
f(...) reprents the 1D convolution

Y.J. Huang, Z. Meng, L.G. Pang, X.N. Wang, arXiv:2504.00790

Classification accuracy

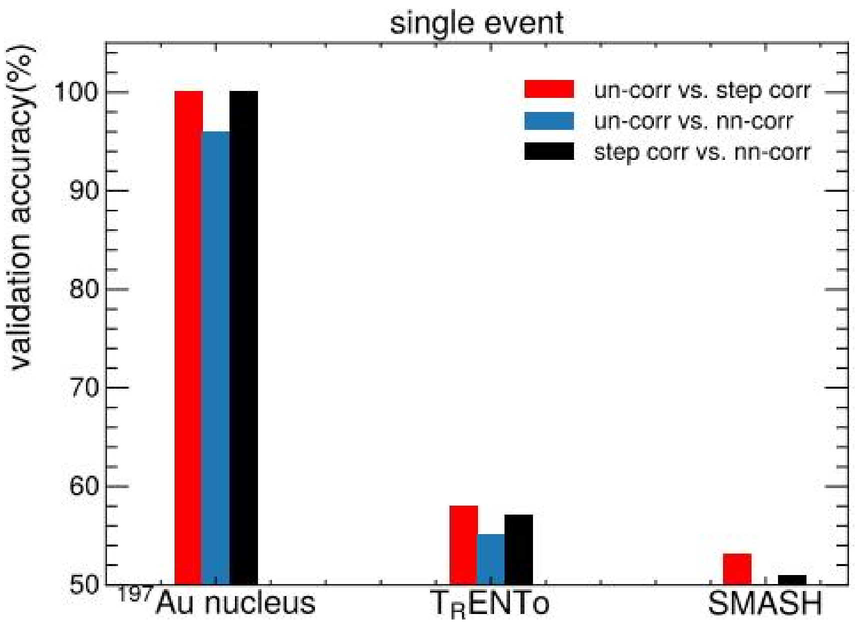

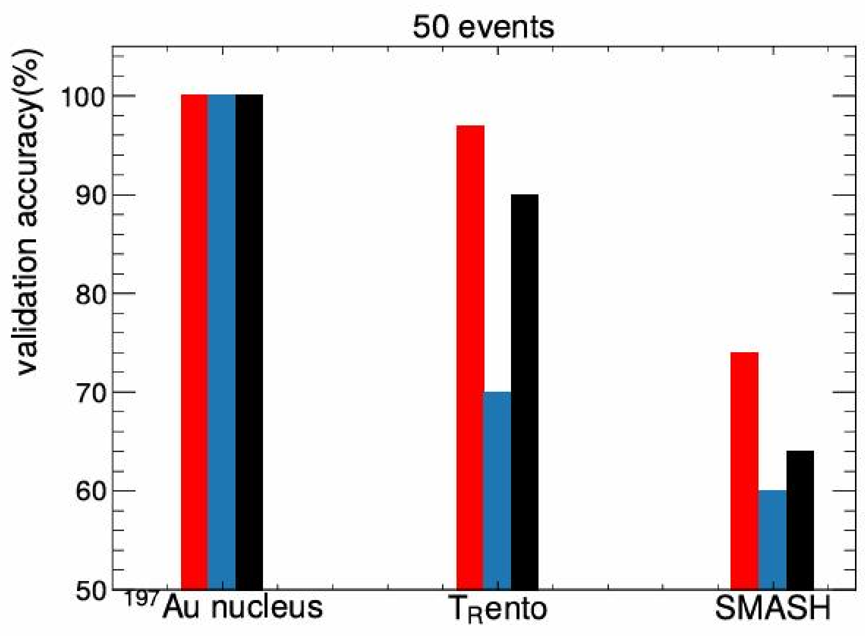

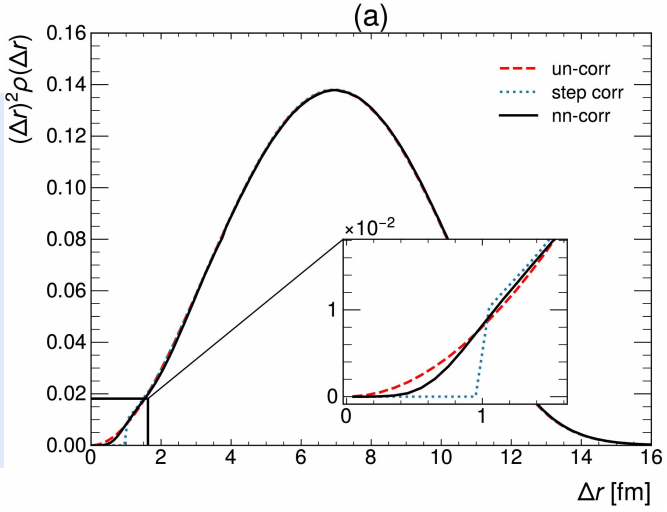

Accuracies

- ➢ lowest for un-corr vs nn-corr
- ➢ Decreases: Initial nucleus → Trento → SMASH
- ➢ Indicating information loss during dynamical evolution

Bayesian analysis QCD EoS

The c_s^2 is parameterized as a function of energy density in the following,

$$c_s^2(\epsilon) = c_s^2(\epsilon_h) + \left(\frac{1}{3} - c_s^2(\epsilon_h)\right) \frac{X_0 x + x^2}{X_0 x + x^2 + X'^2} \tag{2.12}$$

where $X_0 = \sqrt{12} R X' c_s(\epsilon_h)$, $x \equiv \ln \frac{\epsilon}{\epsilon_h}$, ϵ_h is the energy density at $T = 165$ MeV, R and X' are the two parameters in the EoS to be determined. Randomly choosing R and X' from the range $-0.9 < R < 2$ and $0.5 < X' < 5$ generate the unconstrained EoS that varies in a large region between $c_s^2 = 0.05$ and $c_s^2 = 0.33$, as shown in Fig. 2.4-a. This corresponds to the a priori distribution of c_s^2 parameters together with other 12 parameters in the model $P(\theta)$.

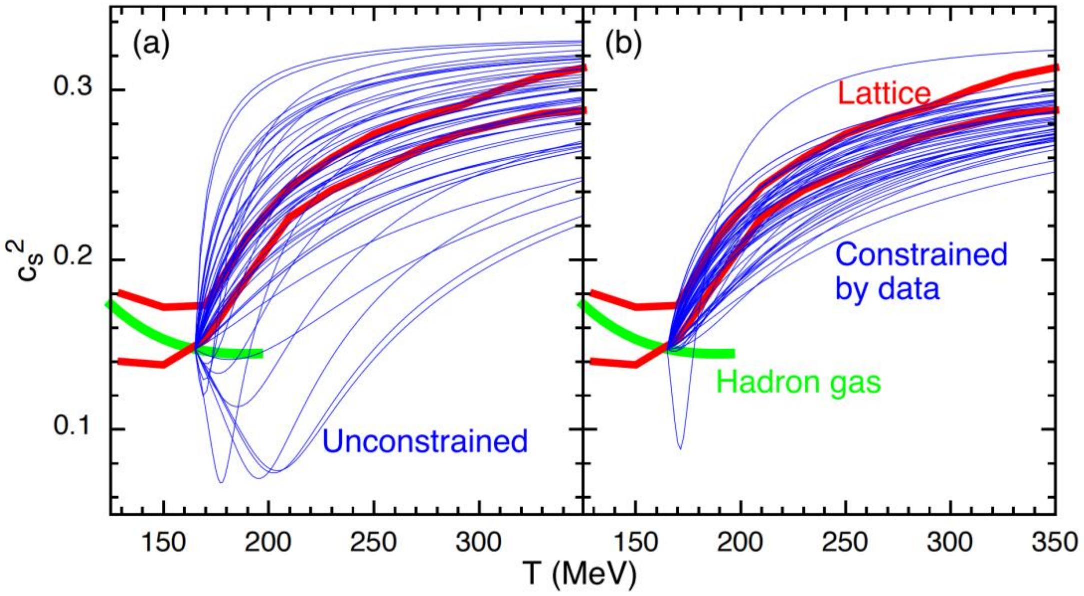

Likelihood: $$P(D|\theta) = \Pi_i \exp\left(-(z_i(\theta) - z_{i,\exp})^2/2\right)$$

Posterior: $$P(\theta \mid D) \propto P(D \mid \theta) P(\theta)$$

S. Pratt, E. Sangaline, P. Sorensen, H. Wang, PRL. 114 (2015) 202301.

Global fitting with Bayesian analysis

Trento + iEBE-VISHNU + UrQMD

TABLE I. Input parameter ranges for the initial condition and hydrodynamic models.

Parameter	Description	Range
Norm	Overall normalization	100–250
p	Entropy deposition parameter	-1 to $+1$
k	Multiplicity fluct. shape	0.8–2.2
w	Gaussian nucleon width	0.4–1.0 fm
η/s hrg	Const. shear viscosity, $T < T_c$	0.3–1.0
η/s min	Shear viscosity at T_c	0–0.3
η/s slope	Slope above T_c	0–2 GeV^{-1}
ζ/s norm	Prefactor for $(\zeta/s)(T)$	0–2
T_{switch}	Particlization temperature	135–165 MeV

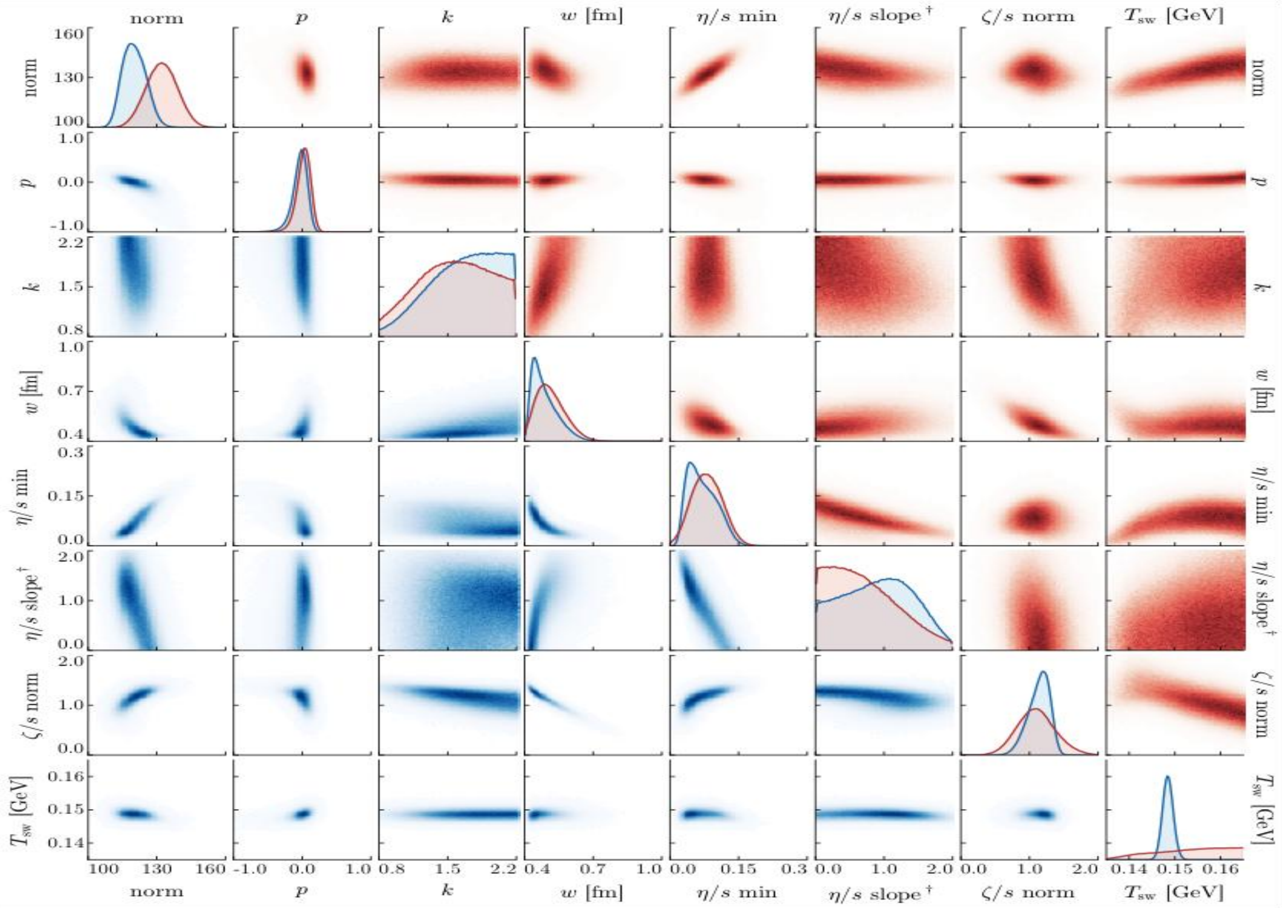

FIG. 7. Posterior distributions for the model parameters from calibrating to identified particles yields (blue, lower triangle) and charged particles yields (red, upper triangle). The diagonal has marginal distributions for each parameter, while the off-diagonal contains joint distributions showing correlations among pairs of parameters. †The units for η/s slope are $[\mathrm{GeV}^{-1}]$.

PRC 94.024907, J. E. Bernhard, J. Scott Moreland, S. A. Bass, J. Liu, U. Heinz

Nature Physics 2019, J. E. Bernhard, J. Scott Moreland, S. A. Bass

Active learning to map out unphysical EoS

$$(\mu_{BC}, \alpha_{\rm diff}, w, \rho) \mapsto P(T, \mu_B) \mapsto \{\text{acceptable, unstable, acausal}\}.$$

4 parameters from 3D Ising model

QCD EoS

Lables for classification

Acceptable = Stable + Causal

$$P, s, \varepsilon, n_B, \chi_2^B, \left(\frac{\partial S}{\partial T}\right)_{n_B} > 0\,,$$

$$0 \le c_s^2 \le 1.$$

D. Mroczek, M. Hjorth-Jensen, J. Noronha-Hostler, P. Parotto, C. Ratti, and R. Vilalta, PRC 107, 054911

Active learning

Achieve high performance with much fewer data (O(10^2))

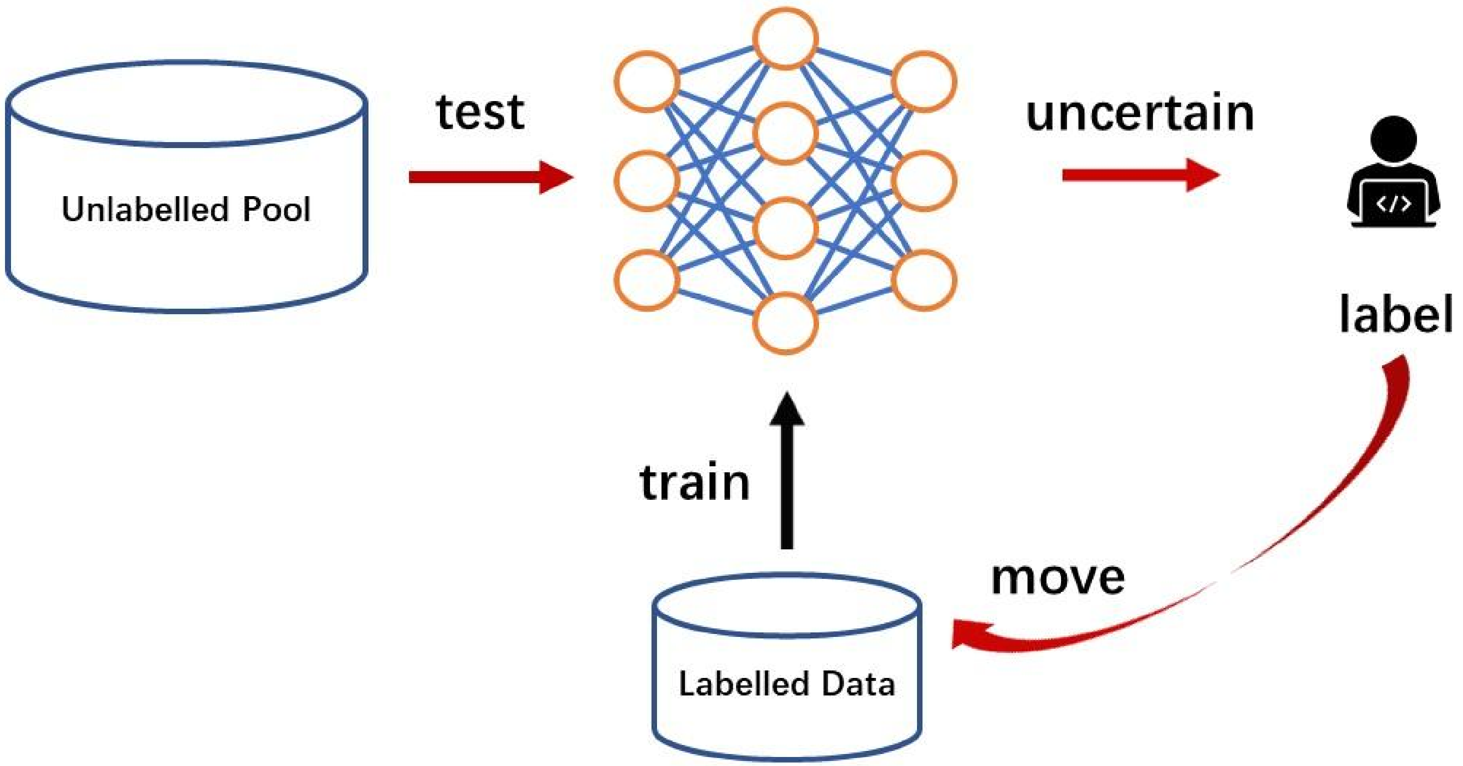

D. Mroczek, M. Hjorth-Jensen, J. Noronha-Hostler, P. Parotto, C. Ratti, and R. Vilalta, PRC 107, 054911

RL for beam control in accelerator

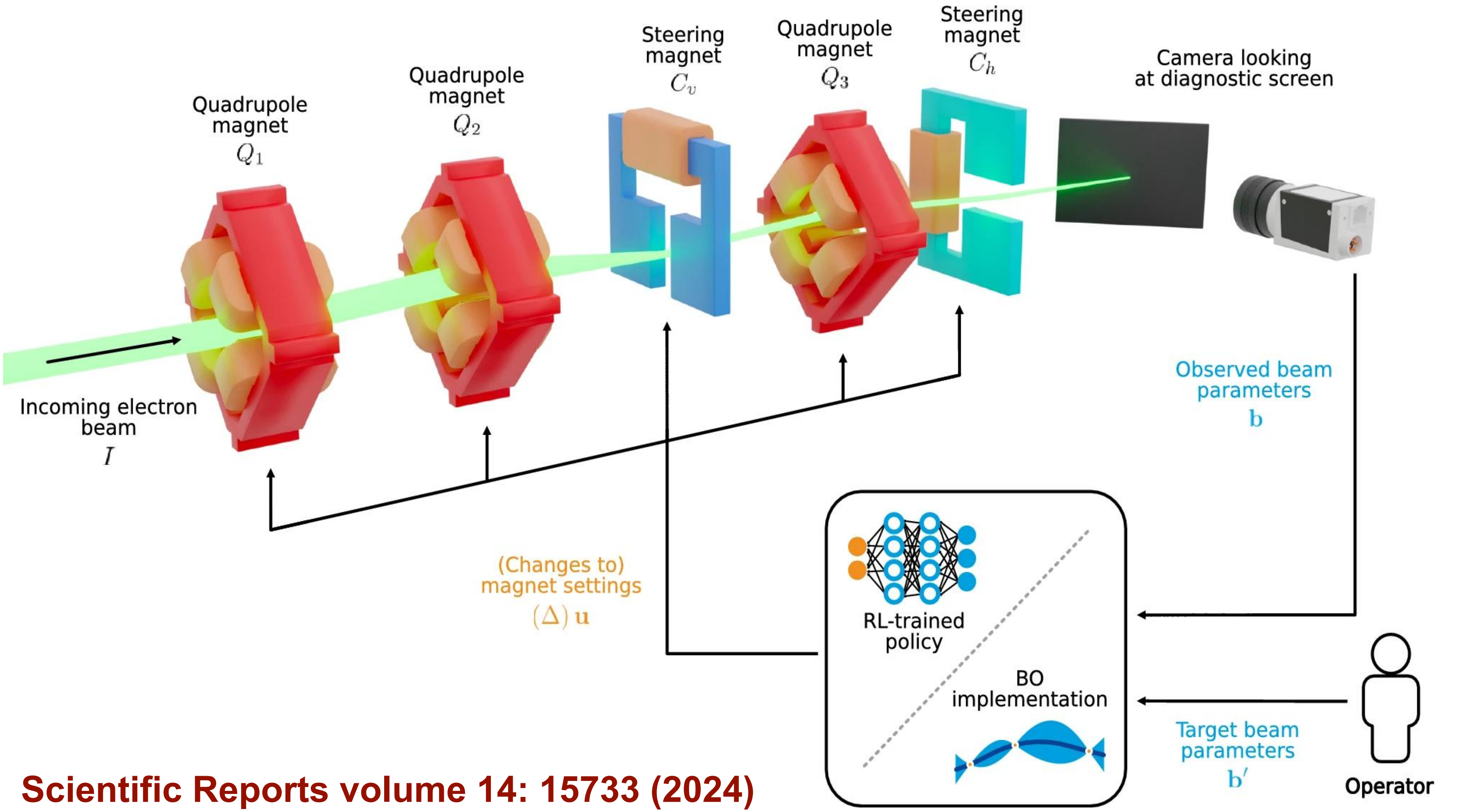

Scientific Reports volume 14: 15733 (2024)